DEVELOPMENT OF AMPHIPHILIC BIODEGRADABLE PHOTOLUMINESCENT POLYMERS

by

SHENGYUAN ZHOU

Presented to the Faculty of the Graduate School of
The University of Texas at Arlington in Partial Fulfillment
of the Requirements
for the Degree of

MASTER OF SCIENCE IN MATERIAL SCIENCE AND ENGINEERING

THE UNIVERSITY OF TEXAS AT ARLINGTON
August 2010

ACKNOWLEDGEMENTS

I am very appreciated my advisor Dr. Jian Yang for providing me such a wonderful opportunity to work in his laboratory, and for his guidance and support. His constant motivation, guidance, and inspiration have helped and teach me how to become a better researcher during my years at UTA. I would also like to thank Dipendra Raj Gyawali for his help in working with me on my thesis and other research works.

I would like to thank Yi Zhang for his valuable discussions and help on my research works. I also want to thank Richard T. Tran for his advice and modification on my manuscript of thesis. I would like to extend my appreciation to my coworkers and friends, Aleksey Kolasnikov, Parvathi Nair, et al. for their continuous inspiration and encouragement. I would also like to thank the lab members from Dr. Nguyen's lab for allowing me to use their laboratory facilities.

Finally, I would like to thank my parents for their patience, their support, their love and their encouragement.

July 16, 2010

ABSTRACT

DEVELOPMENT OF AMPHIPHILIC BIODEGRADABLE

PHOTOLUMINESCENT POLYMERS

Shengyuan Zhou M.S.

The University of Texas at Arlington, 2010

Supervising Professor: Jian Yang

The development of amphiphilc block copolymers have attracted much attention due to their potential uses in drug delivery and targeting. Very few researches are focused on their prospective applications as fluorescent imaging probes. Although some researcher have reported that fluorescent materials encapsulated in amphiphilc micelles could provide significant opportunities for biological labeling and imaging in biomedical fields, these fluorescent materials, such as organic dyes and quantum dots, suffer from photobleaching, cytotoxicity and lack of biodegradability. A novel and ideal amphiphilic biodegradable photoluminescent polymeric micelle should open new avenues for drug delivery and bioimaging.

The objective of this research was to develop novel biodegradable photoluminescent amphiphilic block polymer (BPABP), comprised of a photoluminescent hydrophobic block, poly(propylene glycol)- citrate-cysteine) (PPGCA-Cys), and a hydrophilic block, poly(ethylene glycol) (PEG). Such photoluminescent polymeric micelles with various block compositions were successfully prepared and characterized using Fourier transformed infrared spectrometer (FTIR), nuclear magnetic resonance (NMR), ultra violet-visible spectrophotometer and fluorospectrophotometer. The results of photoluminescent properties of polymeric micelles supported that BPABP offers advantages over the traditional polymeric micelles due to their unique photoluminescent properties. These photoluminescent properties can be tuned by varying the molecualar weight of hydrophobic component of amphiphilic polymers and the choices of monomers, specifically amino acids. Also, the cytotoxicity evaluation indicated a superior in vitro biocompatibility compared to semiconducting quantum dots. The results from dynamic light scattering (DLS) and transmission electron microscopy (TEM) indicated the size range of these micelles were from 120 to 180 nm. The critical micelle concentration (CMC) was varied with the change of hydrophobic chain length. The drug loading efficiency and release behavior in vitro justifiedtheir potential uses as drug vehicle. Lastly, we demonstrated the possibility of using BPABPP micelles for in vitro cellular labeling. Therefore, the development of novel BPABP micelle can offer new opportunity in bioimaging and drug delivery.

TABLE OF CONTENTS

LIST OF ILLUSTRATIONS

Figure Page

LIST OF TABLES

CHAPTER 1

INTRODUCTION

As effective drug delivery vehicles, the applications of amphiphilic micelles have been investigated and reported during last 30 years [1-10]. Also, the development of fluorescent organic and inorganic materials created new fields based on their potential uses and unique photoluminescent properties in various fields including lighting industries [11-15]. Moreover, recently, the fluorescent materials encapsulated in amphiphilc micelles brought significant opportunities for biological labeling and imaging in biomedical fields. In this chapter, an overview on self-assembly principles of micelles, advantages of micelles as drug carriers, applications of commonly used fluorescent materials (organic dyes, fluorescent protein and quantum dots), and disadvantages of currently used fluorescent material-encapsulated micelles will be discussed.

1.1 Polymeric micelles

1.1.1 Self-assembled Principle of Micelles

In recent years, micelles formed from amphiphilic block copolymers have attracted significant attention in various medical and biological fields as potential carriers for genes and hydrophobic drugs [1-3]. The unique behavior of amphiphilic polymeric molecules can be

attributed to the presence of hydrophilic and hydrophobic segments, which have a tendency to accumulate at the boundary of two phases. [4-9]. Micelles can be formed spontaneously due to a balance between entropy and enthalpy. The self-assembly of amphiphilic block copolymers in water is driven by hydrophobic interactions among the hydrophobic core-forming polymer chains. At a low concentration, , polymer chains of the amphiphilic polymers are fully relaxed in an aqueous solution. As the concentration of the amphiphilic polymers is increased, a point is reached at which the unfavorable entropy condition, named as critical micelle concentration (CMC), derived from the hydrophobic components of the polymer, become dominant. At this point, the hydrophobic chains of a portion of the amphiphilic block copolymers must be withdrawn from the aqueous media [10]. Therefore, the amphiphilic molecules spontaneously start to form micelles (Fig 1.1).

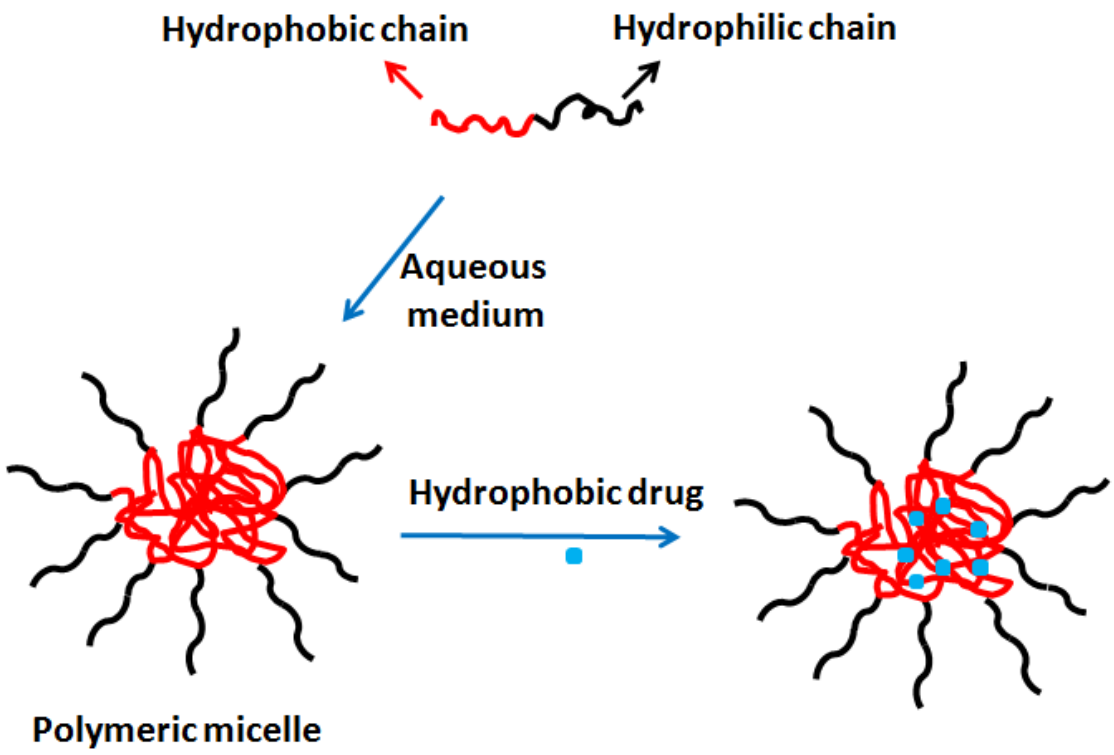

Fig 1.1 The self assembled micelles and encapsulation of drugs

1.1.2 Advantage of Polymeric Micelles

It is well known that amphiphilic block copolymers are able to spontaneously self-assemble into polymeric aggregates including micellar and vesicular conformations in aqueous environment. The hydrophilic corona provides relative stable interface for micelles while the hydrophobic inner core can encapsulate hydrophobic drugs. Based on its amphiphilic behavior, many industrial applications of block copolymeric micelles have been reported, such as detergents, emulsifiers, dispersants, foaming agents, solubilizers, etc [16-19]. Also, the CMC values of

amphiphilic polymers are much higher than those of typical small molecule surfactant [26]. This optimal feature provides potential stability of micelles in extremely dilute state of biological fluids. Therefore, polymeric micelles can be used as efficient carriers for reagents with poor solubility and low stability in aqueous environment. In addition, polymeric micellar aggregates have received much attention as drug delivery carriers for various anticancer drugs, due to the enhanced permeation and retention (EPR) effect of particles in tumor tissues. According to Allen et al. [20], the size of polymeric micelles less than 200 nm in size, have the ability to reduce non-selective uptake by the reticuloendothelial system (RES). Therefore, the polymeric micelle carrier system not only improves the targeting efficiency to tumor tissues, but also becomes ideal drug delivery carriers, maintain relatively low CMC, slow disassemble rate, and nontoxic degradation products.

1.1.3 Conformation and Stability of Micelles

For preparation of micelles, linear diblock copolymer, triblock copolymers and block copolymers with more complex architectures have been explored as delivery systems in recent years [21, 22, 27-29]. The mostly used hydrophobic blocks are polyesters (e.g. polycaprolactone (PCL), poly(d, l-lactide) (PDLLA)), polyethers (e.g. poly(propylene oxide) (PPO)) or polyamino acids (e.g. poly(b-benzyl-l-aspartate) (PBLA)); while the hydrophilic polymer block is usually poly(ethylene glycol) (PEG) [23-25], because PEG is an excellent biocompatible biomaterial due to its hydrophilicity, flexibility and nontoxicity. However, polymeric micelles provide thermodynamic

stability only above the CMC. When the concentration drops below the CMC, the micellar structures become unstable and dissociate into free polymer chains. For in vivo drug delivery application, the thermodynamic instability of the micelles below the CMC should be considered and evaluated, because the micelles suffer from severe dilution after entry into the bloodstream. Once the burst release of entrapped drugs cannot be avoided due to low CMC of micelles, the large fluctuations of drug concentrations may cause serious toxicity problems [26]. In order to overcome this drawback, a series of multi-arm star amphiphilic block copolymers (SABCs) with a hydrophobic multi-arm core and large number of amphiphilic arms were reported as hydrophobic drug delivery carriers [27-29]. Wang et al. reported multi-arm SABCs with a large number of arms by ring-opening polymerization of caprolactone and L-lactide using polyamidoamide (PAMAM) as the macroinitiator followed by coupling with poly(ethylene glycol) (PEG) [27]. The coexistence of unimolecular micelles and larger micelle aggregation was observed in an aqueous medium [27-29]. In addition, cross-linking of the shell or core of hydrophobic micelles is another potential stratagem to improve the stability of micelles and was confirmed by a decrease or even the absence of a CMC [30]. Shuai et al. explored core cross-linking of paclitaxel-loaded PEG-b-PCL micelles by radical polymerization of double bonds introduced into the PCL blocks [31]. These micelles exhibited remarkable enhanced thermodynamic stability against dilution with aqueous medium.

1.1.4 Drug Loading in Block Copolymer Micelles

The three most commonly used drugs in block copolymer micelle systems are doxorubicin hydrochloride (DOX), paclitaxel (PTX) and 5-fluorouracil (5-Fu). DOX has been successfully loaded into poly(ethylene glycol)-b-poly(l-lactic-co-glycolic acid) (PEG-b-PLGA) [32], poly(ethylene glycol)-b-poly(caprolactone) (PEG-b-PCL) [33] and poly(ethylene oxide)-b poly(propylene oxide)-b-poly(ethylene oxide) (PEO-b-PPO-b-PEO) copolymer [34]. PTX has been incorporated into copolymers such as PEG-b-PCL [35] and poly(ethylene glycol)-b-poly(d, llactide) (PEG-b-PDLLA) [36]. 5-fu has been encapsulated in copolymer such as star-branched PEO–PLA copolymers [37] and multi-arm star H40-PCL-b-MPEG copolymers [29]. The successful encapsulation of these drugs in various micelle systems demonstrates the suitability of micelles for delivery of drugs having a wide range of physical and chemical properties. However, based on their different water solubility (5-fu has water solubility of 10 mg/mL and water solubility of PTX is only 1 μg/mL), the drug release profile exhibited significantly differences in in vitro study. Pan et al. reported anti-cancer drugs 5-FU and PTX were loaded into star-branched PEO–PLA micellar nanoparticles [37]. Triblock, diblock and starshaped copolymers were compared for 5-fu release. All showed very little control over the release. 5-fu was rapidly released in vitro within 30 h, while the release of PTX from these polymers could be controlled over 2 weeks.

1.1.5 In vivo Release of Drugs from Block Copolymer Micelles

Recently, polymeric micelles have been investigated as an effective anticancer drug delivery system for cancer chemotherapy. Yuan et al. reported water-insoluble drug ATRA-loaded PEG–PLA diblock copolymer micelles showed longer circulation time in blood than ATRA solution in vivo [38]. It might be the result of the PEG corona which could prevent the adsorption of plasma opsonins (e.g. immunoglobulin, IgG) so that the nanoparticles could be removed slower from circulation by the phagocytic cells of the RES. In order to evaluate anti-tumor efficacy of DOX in vivo, Jinyoung et al. compared free DOX, pH-sensitive polymeric micelles, and DOX-loaded/pH-responsive polymeric micelles in B16F10 tumor-bearing mice [39]. DOX-loaded/pH-responsive polymeric micelles showed visible antitumor efficacy, and enhanced survival rates, compared with free DOX. All the results promised future for injection administration.

1.2 Fluorescent Materials

1.2.1 Organic Dyes

Organic dyes were considered to be useful fluorescent label for bio imaging applications, since it contained specific capacity of absorbing and emitting visible light [40]. Chromogen is the aromatic structure containing benzene, naphthalene, or anthracene rings. A chromophore group is a color provider and is characterized by the following radicals which confirm a basis for chemical

classification of dyes. Nitro, nitroso, azo, sulfur, carbon-nitrogen dyes are the most commonly used dyes. In biological field, as novel optical reporters and imaging probes, organic dyes had a broad application, including cellular and molecular imaging and tracking, multiplexed analyses, and DNA detection [40-41]. However, most organic dyes have limitations and drawbacks, particularly in multicolor experiments and in vivo studies due to problems associated with signal intensity strength, poor photostability, relatively short fluorescence lifetime, narrow excitation spectra and broad emission ranges [41]. These problems limited their applications in biological and biomedical fields.

1.2.2 Fluorescent Proteins

As fluorescent labels, fluorescent proteins, such as green fluorescent protein (GFP), blue fluorescent protein (BFP), red fluorescent protein (RFP) et al, were developed. Today, GFP and its mutations have been widely used in almost all organisms and all major cellular compartments [11, 12]. In cellular biology, GFP has been used as a cell marker, a fusion tag, a gene indicator, a calcium sensor, and an active indicator for protease action. Unfortunately, during prolonged illumination, almost all organic fluorescent materials including fluorescent proteins suffer from irreversible photobleaching,. In addition, fluorescent proteins by themselves are not used as drug carriers in drug delivery.

1.2.3 Fluorescent Quantum Dots

The development of fluorescent quantum dots (QDs) have triggered new interest because of their unique chemical and optical features. [42]. In order to dramatically improve their uses in long-term, multi-targeted, and highly sensitive imaging applications in cancer therapy and diagnosis, QD technology has become one of the most exciting and fastest growing applied technology [43, 44]. In comparison to organic dyes, QDs possess attractive properties for biologists which include high molar extinction coefficients (~10–100× that of organic dyes), high quantum yields, and broad excitation spectrum with narrow emission bands with mostly symmetric spectra shape. Therefore, many groups have focused on the use of QDs as fluorescent imaging probes for biological applications. However, the inherent toxicity of semiconducting QDs limits their uses in biomedical fields.

1.2.3 Fluorescent Quantum Dots

The development of fluorescent quantum dots (QDs) have triggered new interest because their unique chemical and optical features, which have the potential to function as unique photoluminescent markers for cell and a variety of biological investigations [42]. In order to dramatically improve the use of long-term, multi-targeted, and highly sensitive imaging applications in cancer therapy and diagnosis, the use of fluorescent quantum dots in biology has

become one of the most exciting and fastest growing applied technology [43, 44]. I In comparison to organic dyes, QDs possess attractive properties for biologists which include, high molar extinction coefficients (~10–100× that of organic dyes), high quantum yields, and broad excitation spectrum with narrow emission bands of mostly symmetric shape. Therefore, more groups have focused on the use of semiconductor nanocrystals (QDs) as fluorescent imaging for biological applications.

1.3 Disadvantage of Fluorescent Materials Encapsulated in Micelles

There has been a significant interest in developing biodegradable photoluminescent amphiphilic block copolymer within past few dacades. In previous works, photoluminescent properties of fluorescent organic dyes and QDs were investigated for characterizing target-specific delivery of micelles though bioimaging [45, 46]. Especially, by encapsulting organic dyes 1,8-anilinonaphthalenesulfonate (ANS), poly(styrene-b-2-(N,N-dimethylamino)ethyl methacrylate) diblock copolymers formed stable micelles at extremely low polymer concentrations with fluorescent properties [47]. Water-soluble CdSe-ZnS nanocrystals (QDs) [43], encapsulated within an amphiphilic block polymer, were used for multiphoton imaging in biological environments, such as the skin of living mice. The use of near-infrared QDs enables imaging at greater depths as compared to the use of standard fluorophores. However, the drawbacks of organic dyes and QDs are not addressed in such systems. [44] Currently, there are no biodegradable amphiphilic block

copolymer micelles which can inherently emit detectable fluorescent signals for biological labeling and imaging. Therefore, there is an urgent need for the development of biodegradable and biocompatible photoluminescent amphiphilic block copolymer micelles.

1.4 Aliphatic Biodegradable Photoluminescent Polymers

Recently our lab has developed aliphatic biodegradable photoluminescent polymers (BPLPs), which emit strong, tunable fluorescence emission ranging from blue to red [48]. In this research, BPLPs were prepared using 1,8-octanediol, citric acid and different amino acids as the monomers. BPLP-serine (BPLP-Ser) emits different fluorescent colors from blue to red with an increased excitation wavelength. To further explore this family of materials, all of the twenty essential amino acids were used separately to make BPLP families. The emission of polymer with polar R-grouped amino acids was found to be more intense than rest of the amino acids. L-cysteine also belongs to the category of polar R-grouped amino acids which showed the highest intensity of emission among twenty amino acids. In addition, by varying the molar concentration of L-cysteine in the polymer, the fluorescence intensity of BPLP-cys can be turned, in which BPLP-cys0.2 exhibited the strongest fluorescent intensity. BPLPs exhibited higher quantum yield and longer fluorescent lifetime as compared to the conventional organic dyes. Also, BPLPs can be used as imaging probes, which showed advantages of degradability, cell compatibility and noninvasive in vitro and vivo study as compared to QDs.

1.5 Innovative Aspects and Aims

1.5.1 Innovative Aspects

As we known, BPLPs have been recognized as biodegradable photoluminescent polymers, which can be used as imaging probes. However, hydrophobic BPLPs can not efficiently encapsulate hydrophobic drugs as drug delivery vehicles. Considering the wide applications and growing attentions of amphiphilic micelles and optical imaging in biological and biomedical fields, herein, we developed novel biodegradable photoluminescent amphiphilic block copolymer (BPABP) micelles. The syntheses of the unique BPABP micelles were based upon the previously reported BPLPs [48]. These novel amphiphilic di-block copolymers comprised of a photoluminescent hydrophobic block, poly(propylene glycol)- citrate-cysteine) (PPGCA-cys), and a hydrophilic block, poly(ethylene glycol) (PEG), were prepared. PEG was utlized as a non-toxic biocompatible outer hydrophilic shell [49, 50]. PEG-based coronas have also been shown to stabilize micelles, and prolong the circulation time in blood for enhanced tumor targeting while also minimizing protein adsorption to decrease nonspecific cell adhesion and uptake. Based on amphiphilic and photoluminescent properties of BPABPs, we try to investigate their potential uses in drug delivery and cellular imaging for cancer therapy and diagnosis. We believe this novel photoluminescent amphiphilic di-block copolymers will open new avenues for bioimaging of drug delivery studies and provide a potential opportunity for cancer therapy and diagnosis due to their

tunable fluorescence emission, high quantum yield, degradability, photostability, themodynamic stability of micelles, low CMC and cell compatibility.

1.5.2 Specific Aims

- Aim 1: Synthesis and characterization of amphiphilc block copolymer
- Aim 2: Investigation of micelle properties and photoluminescence properties
- Aim 3: Bioimaging , cytotoxcity and drug delivery study in vitro

CHAPTER 2

EXPERIMENTAL

2.1 Materials

All the chemicals required for this project were purchased from Sigma Aldrich (St. Louis, MO) unless otherwise stated. All chemicals were used without further purification.

2.2 Methods

2.2.1 Poly(propylene glycol-co-citrate)-cysteine (PPGCA-cys) Synthesis

PPGCA-cys was prepared through a simple condensation reaction by citric acid (CA), poly(propylene glycol) (PPG), and L-cysteine in a 1.0:1.1:0.2 molar ratio, respectively (Fig.1). Briefly, PPG, CA, and L-cysteine were added to a 100 mL round bottom flask, and melted by stirring at 160 ºC. Once all the contents had melted, the temperature of the system was lowered to 140 ºC, and allowed to react for several hours under vacuum to obtain pre-PPGCA-cys. In order to prevent pre-polymer crosslinked, this reaction should be stopped stirring at 120 RPM. Next, the prepolymer was dissolved in 1,4-dioxane, and purified by drop-wise addition into deionized water under constant stirring. Finally, the purified pre-PPGCA-cys was collected and dried using lyophilzation for 2 days. In order to study the effect of the hydrophobic segment size on the

resulting micelle properties, PPG 425, 725, and 2000 Da were used. Actually, PPG 2000Da takes long time to conjugate with citric acid in this reaction, actually the molar ratio of P

PG 2000Da and citric acid should be 1:1.4

2.2.2 Synthesis of Carboxylic Acid-terminated Methoxy Poly(ethylene glycol) (MPEG-COOH)

Carboxylic acid-terminated methoxy poly(ethylene glycol) (MPEG-COOH 750) was prepared via an esterification process (Fig. 1) [51]. Briefly, MPEG750 (10 g) was dissolved in anhydrous toluene (200 mL) using a 500 mL round bottom flask. Next, succinic anhydride (2.0 g, 0.020 mol) was added, and the reaction mixture was refluxed at 150 ℃ for 10 h. After the solution cooled down, the residue was filtered out, and the remaining toluene was distilled under reduced pressure. Next, the polymer dissolved in 20 mL hot water (70 ºC). The collected organic phase was then dried with anhydrous Na_2SO_4, stirred overnight, filtered, and distilled under vacuum. Then, 20 mL dry ethyl ether is added dropwise into the 3ml $CHCl_3$ polymer solution, and the top layer of ethyl ether was thrown away. This extraction process was repeated three times. The collected organic phase was dried under vacuum.

2.2.3 Preparation of Amphiphilic Diblock Copolymer BPABP (PPGCA-cys0.2-MPEG)

Briefly, 2.5 mmol three different PPGCA-cys0.2 (PPG Mn of 425, 725, and 2000 Da, respectively), 2.5 mmol MPEG-COOH, 0.5 mmol of N-dimethyl aminopyridine (DMAP), and 10

mmol of dicyclohexyl carbodiimide (DCC) as a coupling agent were added to 100mL round bottom flask conatining 50 mL of 1,4-dioxane at room temperature while stirring and maintained for 24 h. After one day the precipitated dicyclohexylurea (DCU) by-product was filtered, and the filtrate was concentrated under reduced pressure and quickly poured into a large amount of cold diethyl ether with vigorous stirring. After filtering under reduced pressure, the product was further placed in a dialysis bag to remove any unreacted MPEG-COOH. After 72h of dialysis, the product was separated out using lyophilization.

2.2.4 Preparation of the Micellar Particles in Aqueous Solution

100 mg of BPLPs(MPEG-b-PPGCA-cys) was dissolved in 5 mL of acetone to make a 2% w/v solution. Then, 200 µl of the 2% w/v polymeric solution is added drop wise into 20 mL deionized water under gently stir. The acetone was allowed to evaporate at room temperature for several hours to produce an aqueous solution of micelles.

2.3 Measurement and Characterization

2.3.1 FTIR and ^{1}H- NMR

For ^{1}H-NMR analysis, 5 mg of purified pre-polymer, and block copolymer BPLPs(MPEG-b-PPGCA-cys) was dissolved in 1 mL of deuterated dimethyl sulfoxide (DMSO-d6). ^{1}H-NMR spectra were collected at room temperature using a JEOL 300 MHz spectrometer. For

Fourier Transform Infrared (FTIR) analysis, purified polymer was dissolved in 1, 4-dioxane to make a 5 wt% solution. The polymer solution was cast onto potassium bromide pellets and the solvent was allowed to evaporate overnight. The FT-IR spectra were recorded at room temperature on a Nicolet 6700 FTIR spectrometer (Thermo Fisher Scientific).

2.3.2 Determination of Critical Micelle Concentration

In order to determine the critical micelle concentration (CMC), fluorescence spectra of the polymer solutions were collected on a Shimadzu RF-5301 PC fluorospectrophotometer at room temperature. Pyrene was used as a hydrophobic fluorescent probe. The pyrene-loaded micelle solution was prepared as following. First, a known amount of pyrene in acetone was added into 10 ml vials and the final concentration of pyrene was 6.0×10^{-7}M which was lower than the saturated solubility of it in PBS (0.5 M, pH 7.4). After the acetone was evaporated, a total of 10 ml of various concentrations of polymer solution were prepared. The ratios of the peak intensities at 338 and 333 nm (I338/I333) of the excitation spectra were analyzed as a function of polymer concentration. The critical micelle concentration (CMC) value was taken from the intersection of the tangent to the curve at the inflection with the horizontal tangent through the point at the low concentrations [52 53].

2.3.3 Micelles particle size and morphology analysis

The hydrodynamic diameter of the MPEG-b-PPGCA-cys micelles (0.2 mg/mL) was measured in water and PBS solution by a dynamic light scattering (DLS) technique using a Nanotrac (Microtrac, Montgomeryville, PA). The morphology of the block copolymer micelles with various concentrations were characterized by TEM (JEOL-1200 EX II). TEM image of the micelles was operated at an acceleration voltage of 80 kV. For TEM studies, a drop of polymeric micelles was deposited onto a 200 mesh copper grid coated with carbon. After the deposition, the aqueous solution was blotted away with a strip of filter paper and dried in air.

2.3.4 Photoluminescence Spectra

Photoluminescence spectra of PPGCA-cys0.2 were acquired on a Shimadzu RF-5301 PC fluorospectrophotometer. The optimal excitation wavelength for each type of micelles solution emission tests was determined as the one that generated the highest emission intensity. In this study, Pre-BPLPs and BPABP (amphiphilic BPLP) families were excited at 360nm, and the excitation and the emission slit widths were set at 1.5nm and 3nm, respectively, for all samples unless otherwise stated.

2.3.5 Photoluminescence Quantum Yield and Molar Absorption Coefficient

The fluorescent quantum yield of the BPABP micelles was measured using the Williams method [54]. The solution was scanned at optimal excitation wavelength. Then, UV-vis absorbance spectrum was collected with the same solution and the absorbance at the optimal excitation wavelength was noted. Then, a series of solutions were prepared with gradient concentration. The absorbance of the each solution should be controlled within the range of 0.01–0.1 Abs units. The fluorescence spectrum was also collected for the same solution in the 10 mm fluorescence cuvette. The fluorescence intensity, which is the area of the fluorescence spectrum, was calculated and noted. Five solutions with different concentrations were measured and the graphs of integrated fluorescence intensity vs. absorbance were plotted. The quantum yields of the BPLPs (PPGCA-cys) families were calculated according to equation (1) where, Φ = quantum yield; Slope = gradient of the curve obtained from the plot of intensity versus absorbance; η = Refractive index of the solvent; x = subscript to denote the sample, and ST = subscript to denote the standard.

$$\Phi_X = \Phi_{ST}\left(\frac{\text{Slope}_X}{\text{Slope}_{ST}}\right)\left(\frac{\eta_X}{\eta_{SF}}\right)^2 \quad (1)$$

Anthracene (Φ= 0.27 in ethanol) was used as a standard. The BPLP polymers were dissolved in

1,4-dioxane and anthracene was dissolved in ethanol. The slit width was kept same for both standard and samples. Absorbance was measured using a SHIMADZU UV-2450 spectrophotometer. The molar absorption coefficient (ε, $L \cdot mol^{-1} \cdot cm^{-1}$) of the BPLPs (PPGCA-cys) families were calculated according to the Beer-Lambert law, $A = \varepsilon cl$. The molar absorption coefficient is a measurement of how strongly a chemical species absorbs light at a given wavelength. All the experiments were carried out in triplicate.

2.3.6 5-FU-loaded MPEG-b-PPGCA-cys Micelles

The drug loading experiment was conducted using the solvent evaporation and nanoprecipitation method. A MPEG-b-PPGCA-cys (20mg) solution in 3.0mL of DMF was mixed with 5mg of 5-fluorouracil (5-FU), a hydrophobic anti-cancer drug, used widely in pharmaceutical research. The mixture was stirred for 2 h in a closed container. 17 ml of deionized water was added dropwise under gentle stirring. Thereafter, the mixture was dialyzed against deionized water using dialysis tubing molecular weight cut-off 500 Da for 24 h. In order to determine the drug loading efficiency, a weighed quantity (25 mg) of drug-loaded micelles solution was prepared in 20 ml deionized water at room temperature based on typical method mentioned before. After high speed centrifugation, the 5-FU in the supernatant was assayed by a SHIMADZU UV-2450 spectrophotometer at a wavelength of 270 nm. All the experiments were carried out in triplicate.

2.3.7 In vitro Drug Release Study

After dialysis, the in vitro drug release study was performed in an apparatus with 100mL phosphate buffer saline (PBS, pH 7.4) at 37 ℃ [55] . 5-FU-loaded MPEG-b-PPGCA-cys micelles were placed in a dialysis bag (Mw cut-off of 500 Da). The dialysis bag was then immersed in the release medium and kept in a horizontal laboratory shaker at a constant temperature (37 ℃). In order to measure the drug release content, samples (1 mL) were removed periodically and an equivalent volume was replaced by the fresh PBS. The amount of released 5-FU was analyzed with a UV-visible spectrophotometer at 270 nm. Absorbance was measured using a SHIMADZU UV-2450 spectrophotometer. The drug release experiments was performed in triplicate for each of the samples.

2.3.8 Cellular Uptake Study

Amphiphilic block copolymers MPEG-b-PPGCA-cys (2000) was used as representative micelle for cellular uptake study. 3T3 mouse fibroblasts are pre-seeded on sterile glass cover slips at a density of 5,000 cells per ml. After the cell is 60% confluent, the cover slip is washed with PBS and transferred to new Petri dish, and incubated with solution of MPEG-b-PPGCA-cys (2000) micelles at 20 μL/ml. After 4h incubation at 37℃, the cells are wa shed by PBS and observed under fluorescence microscope. For longer cell uptake study, after 4h of incubation of cell with

micelle solution, the micelle solution was replace with culture media and incubate until the desire duration and observed under fluorescence microscope.

2.3.9 Cytotoxicity Evaluation

The relative cytotoxicity of amphiphilic block copolymers MPEG-b-PPGCA-cys was evaluated using MTS viability assay against NIH-3T3 cells according to the manufacture protocol. Briefly, 100 µL of 3T3 mouse fibroblasts (5×10^4 cells/ml) in DMEM supplemental medium and 10% fetal bovine serum was culture in a 96-well plate for 24 h at 37º C, 5% CO_2. The culture medium was then removed and supplied with copolymer MPEG-b-PPGCA-cys solutions at different concentrations (0–1 mg/ml) in complete DMEM media. After 24 h of incubation, the medium was replaced by 100 µL of fresh media and 20 µL of MTS stock solution. The cultures were incubated for another 4 h. The absorbance of the water-soluble tetrazolium salt solution was measured at 490 nm using a Microplate reader. The relative cell viability was calculated by the following equation: relative cell viability (%) = (ODtreated/ODcontrol) x 100, where ODcontrol was obtained in the absence of copolymers and ODtreated was obtained in the presence of copolymers.

CHAPTER 3

RESULTS AND DISCUSSION

3.1. Synthesis and Characterization of PPGCA-cys-b-MPEG Block Copolymers

The novel photoluminescent amphiphilic block copolymer BPLP(PPGCA-cys-b-MPEG) was carried out as shown in Fig 3.1. Three types of amphiphilic block copolymers comprising hydrophilic MPEG (MPEG750) and hydrophobic PPGCA-cys (PPG425, PPG725 or PPG2000) were synthesized.

The FTIR analyses of pre-polymer and block copolymer were shown in Fig 3.4. In the spectrum of MPEG-COOH, the peaks located at 1690–1750 cm^{-1} were assigned to carbonyl (C=O) groups from succinic acid and the bands located at 2877 cm^{-1} corresponded to the $–CH_2–$ of MPEG. A stronger peak at 1112 cm^{-1} assigned to the C–O–C was attributed to PEG ether unit. A relatively broad peak at 3400 cm^{-1} was assigned to -OH group. In the spectrum of PPGCA-cys0.2, the bands at 2877 cm^{-1} and a relatively strong peak at 1112 cm^{-1} were assigned to $–CH_2–$ and C–O–C respectively , which were attributed to PPG unit. And a relatively small peak from the carbonyl (C=O) groups at 1739 cm^{-1} was attributed to CA unit. In the spectrum of the block copolymer PPGCA-b-MPEG-cys, all of these typical absorbing peaks of MPEG-COOH and PPGCA can be detected, thus proving the successful conjugation of the two component blocks in

the block copolymer.

To confirm the successful modification of terminal hydroxyl group present in MPEG to carboxylic group contributed by succinic acid, ^{1}H NMR spectroscopy was utilized. Fig 3.2 displayed the presence of a peak at 3.7 ppm, which was attributed to the proton signals of –OCH_2CH_2– from MPEG. Another characteristic peak at 4.7 ppm was exhibited from MPEG -$C\underline{H_2}$-OH. However, after succinic acid was incorporated into the polymer, a chemical shift to 4.3 ppm was observed, which was assigned to the protons signal of -$C\underline{H_2}$-OCO- from MPEG-COOH. Other characteristic peaks at 2.63 ppm were attributed to protons in $C\underline{H_2}$-COOH from the succinic acid, and the peak located at 12 ppm was attributed to proton signal of -COO$\underline{H}$ from MPEG-COOH. These succinic acid peaks cannot be found in pure MPEG, which also indicated the MPEG-COOH was successfully prepared. In the ^{1}H NMR spectra of PPGCA-cys (Fig 3.3), specific signals were attributed to PPG with 1.15–1.25 ppm ($C\underline{H_3}$, proton k); 3.41–3.45 ppm (CH, proton i); 3.52–3.62 ppm (CH_2, proton “h” attached to the ether group) and multiple peaks around 2.8 ppm (–$C\underline{H_2}$–) from citric acid were also observed. In the ^{1}H NMR spectra of MPEG-b-PPGCA-cys (Fig 3.3), the specific peak at 3.18 ppm was assigned to the protons of the CH_3O- from the PEG moiety. The characteristic peaks from MPEG-COOH with 2.95 ppm (-$C\underline{H_2}$-COO-, proton “f”) and 4.3 ppm (-$C\underline{H_2}$-OCO-, proton “d”) were also observed from MPEG-b-PPGCA-cys, which indicated MPEG-COOH successfully conjugated with PPGCA via an esterification process.

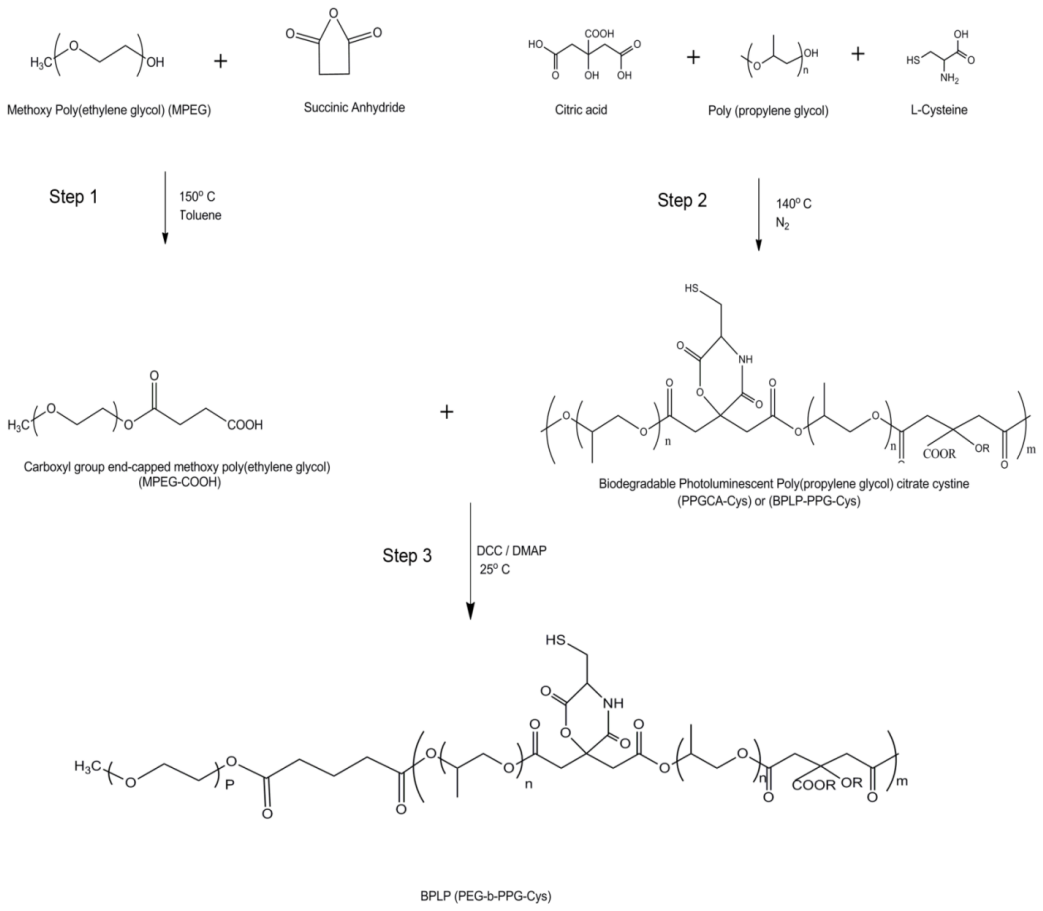

Fig 3.1 Synthesis schematics for BPABP (MPEG-b-PPG-Cys)

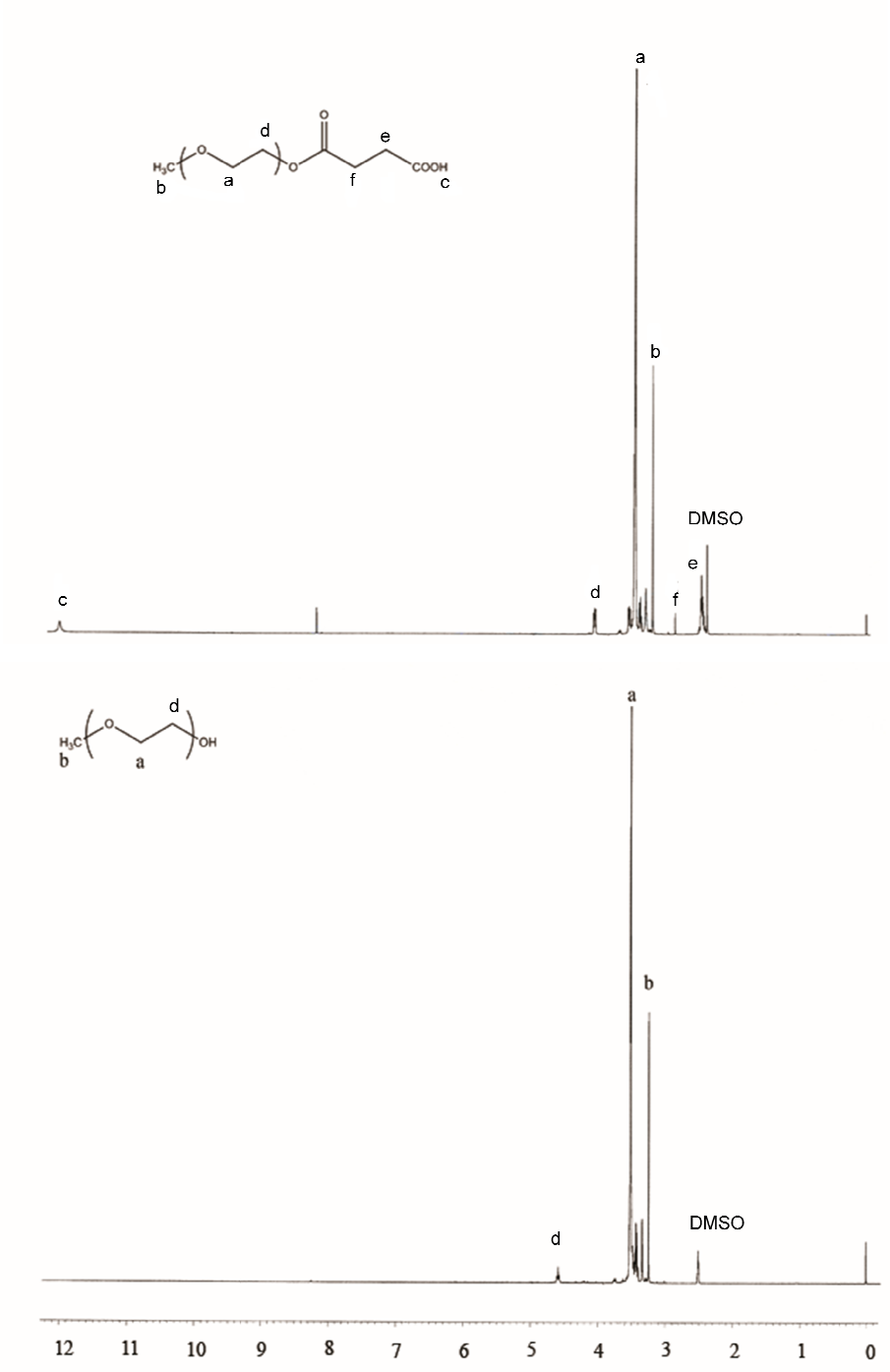

Fig 3.2 ^{1}H NMR spectra of a representative MPEG and MPEG-COOH

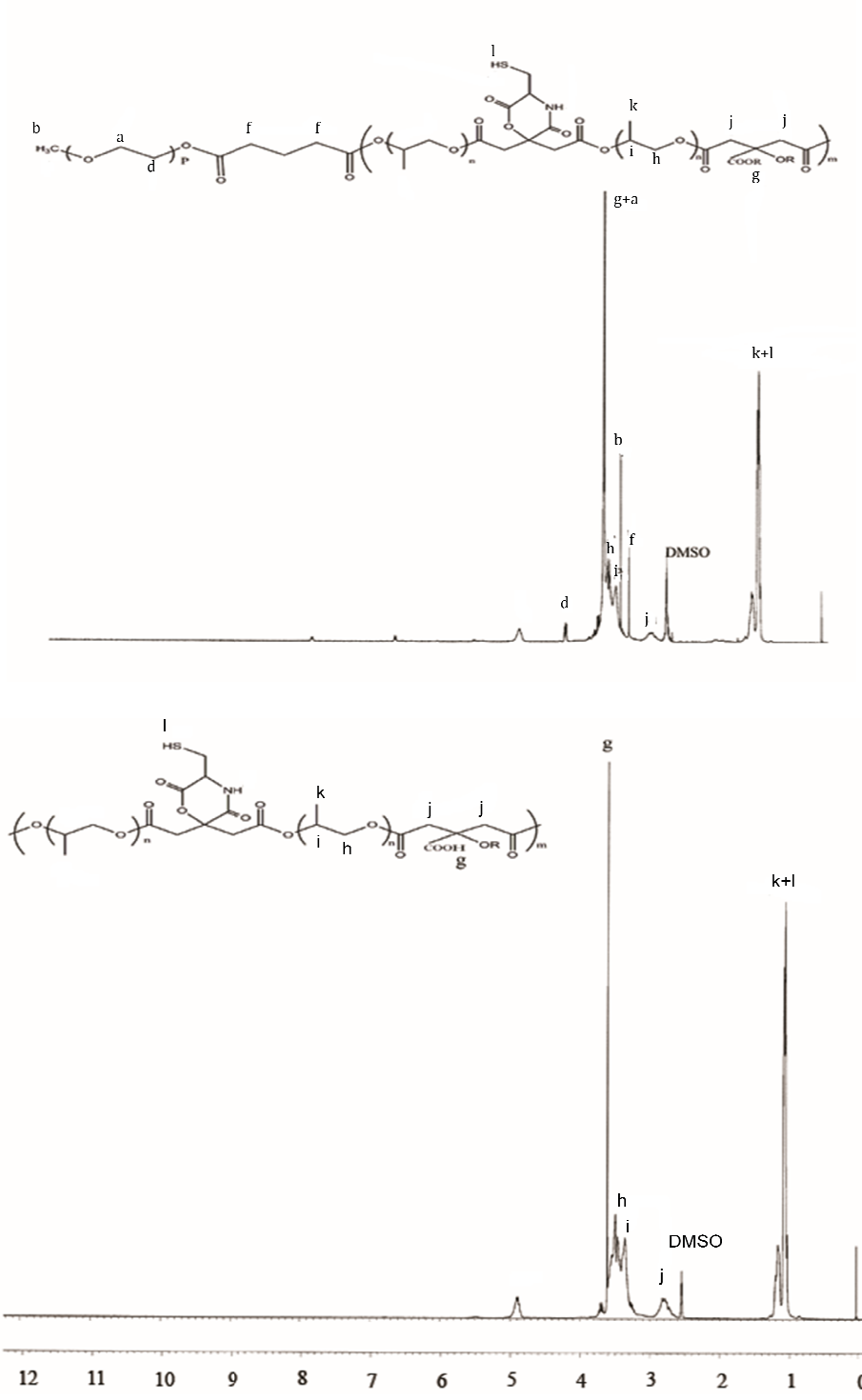

Fig 3.3 ^{1}H NMR spectrum of PPGCA-cys and MPEG-b-PPGCA-cys

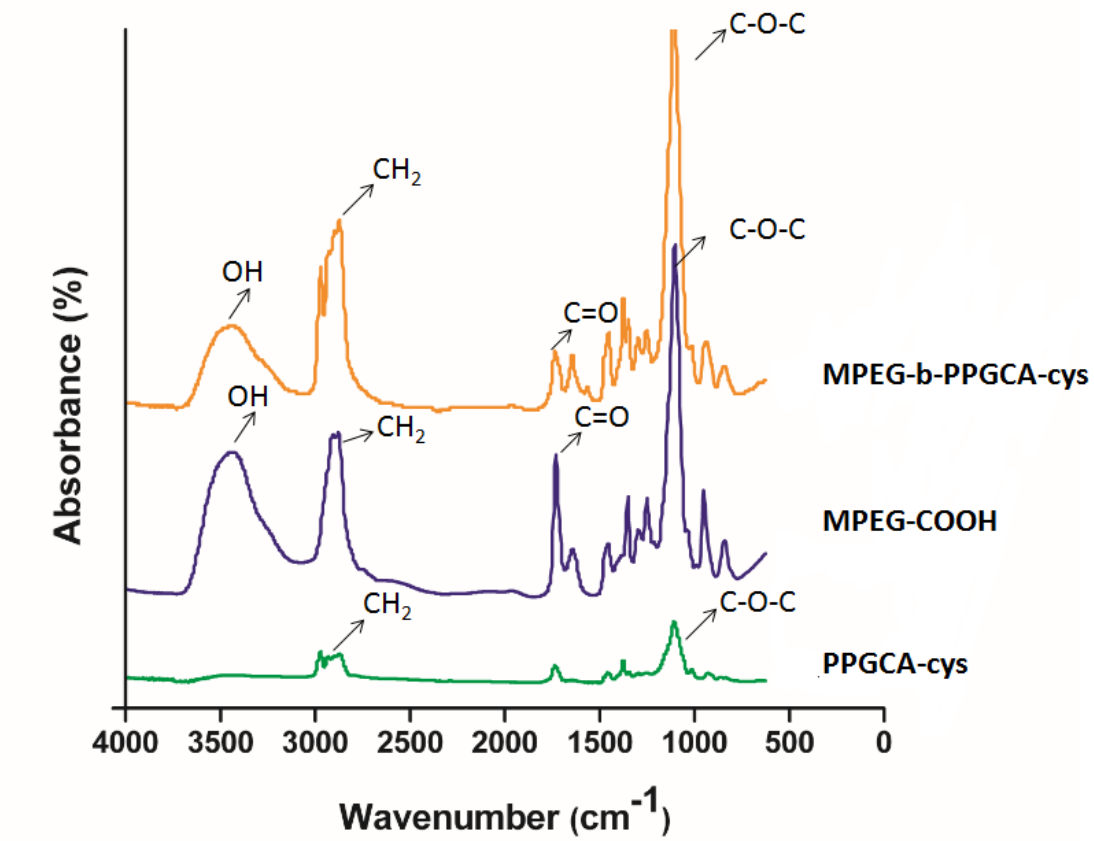

Fig 3.4 FTIR spectra of the MPEG-COOH, PPGCA-cys0.2 and amphiphilic block copolymer MPEG-b-PPGCA-cys

3.2 Critical Micelle Concentrations (CMC)

In order to function as useful long circulating drug delivery vehicles, block copolymer micelles rely on their thermodynamic stability, which is determined by the CMC of the micelles. A low CMC is important to maintain micelle stability and integrity since one of the important differences between the in vitro and in vivo conditions is the effect of dilution after intravenous

administration [56, 57]. Though there are many factors that affect the CMC values of block copolymer micelles, the CMC values of amphiphilic copolymers are heavily determined by the nature of the hydrophobic and hydrophilic blocks as well as their relative lengths. Typically, when the length of the hydrophilic block is held constant, an increase in the length of the hydrophobic block results in a decrease of CMC values [58]. In order to determine the CMC, pyrene was used as a hydrophobic fluorescent probe. Due to the hydrophobic nature of pyrene, the pyrene was incorporated into the hydrophobic core of the polymeric micelles once placed in an aqueous solution. At low concentrations of copolymer, the total fluorescence intensity ratio remained nearly unchanged keeping the normal characteristics of pyrene in a water environment. As the concentration of the copolymer increased, the intensity ratio increased dramatically showing that the pyrene was entirely encapsulated in the hydrophobic environment. In the excitation spectra of pyrene, a red shift from 333 to 338 nm was observed as the block copolymer concentration increased. This is a reflection of the MPEG-b-PPGCA-cys unimolecular micelles aggregation. The CMC was obtained from the intersection of the baseline and the tangent of the rapidly rising I338/I333 curve is shown in Fig 3.5.

In this study, the CMC values of various compositions of photoluminescent amphiphilic block copolymers of MPEG-b-PPGCA-cys were investigated in aqueous solution (Fig 3.5). The CMC value were 7.9, 2.5 and 0.1 mg/L for MPEG-b-PPG425CA-cys, MPEG-b-PPG725CA-cys and MPEG-b-PPG2000CA-cys respectively (Table 3.1), and was shown to decrease as the

fraction of hydrophobic block PPG in amphiphilic copolymers increased indicating that the hydrophobic component played a significant role in the self-assembly behavior of amphiphilic copolymers in aqueous solution [59]. These CMC values were much smaller than those of low molecular weight surfactants, and also smaller than those of most amphiphilic copolymers, such as reported thermo-responsive Biotin-P(NIPAAm-co-NDAPM)-b-PCL with CMC of 36mg/L [60]. The low CMC values indicated that the self-assembled micelles could remain stable in dilute situations such as after intravenous administration, and also aids in the long term stability in the blood systemic circulation. Based on the ‘salt out’ effect [61], an even lower CMC value was expected to exhibit for micelles in ionic blood solution.

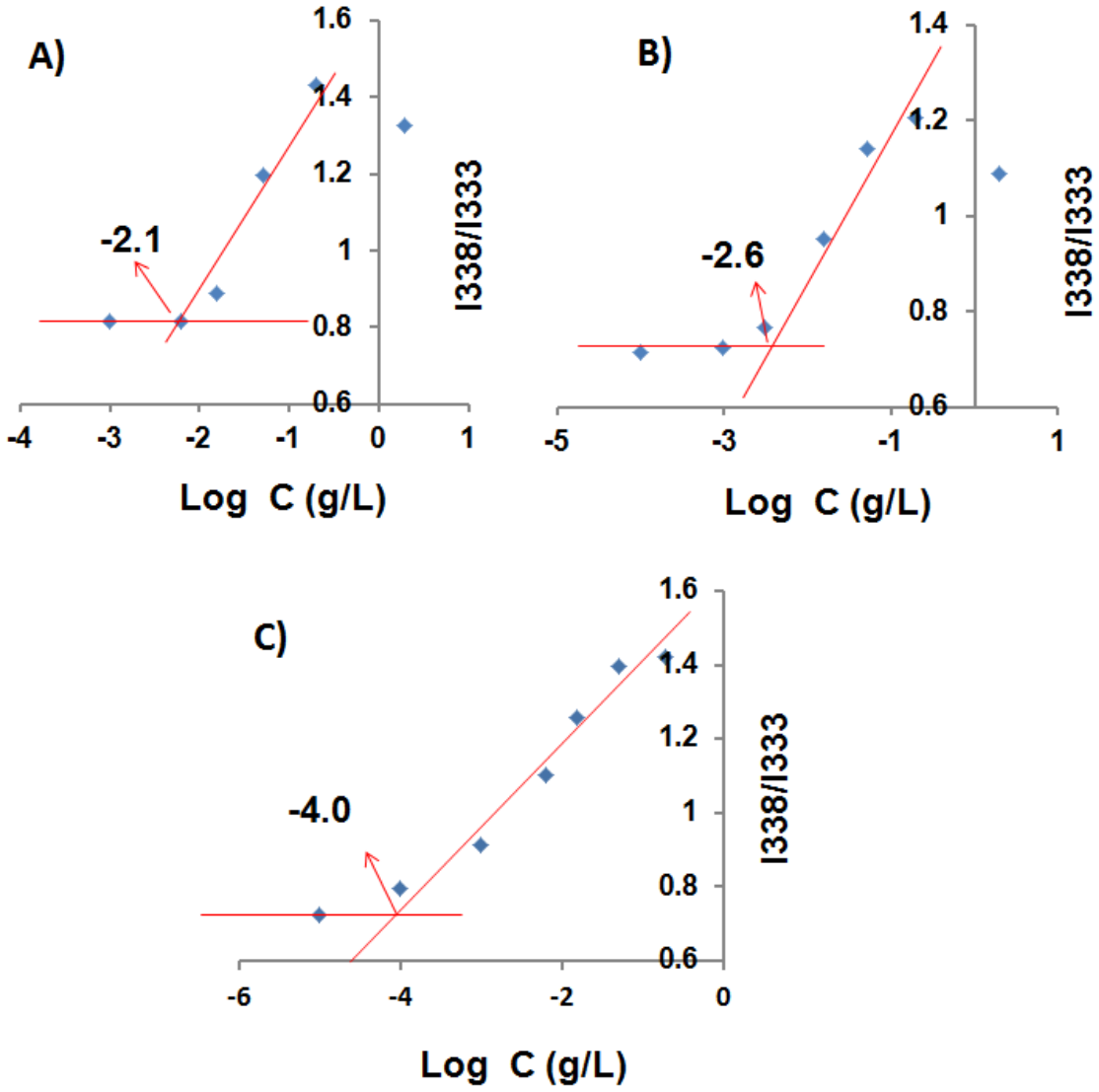

Fig 3.5 Plots of the intensity ratio I338/I333 vs. log C for BPABPs (MPEG-b-PPGCA-cys) with various compositions: (A) MPEG750-b-PPG425CA-cys, (B) MPEG750-b-PPG725CA-cys (C) MPEG750-b-PPG2000CA-cys

3.3 Micelle Particle Size and Morphology Analysis

During the self-assembly process, the amphiphilic block copolymer PPG-b-MPEG-cys spontaneously formed micelles in water in order to minimize the interfacial energy. Transmission electron microscopy (TEM) images show the morphology and sizes of micelles which were prepared by the self-assembly of the BPLPs(MPEG-b-PPG2000CA-cys) copolymer with the concentrations of 0.2g/L (Fig 3.6 A) and 2g/L (Fig 3.6 B). As shown in Fig 3.6, the spherical shape morphology of micelles indicated good self-assembly of the micelles in aqueous solution. As shown in Fig 3.6 (A), when a lower concentration polymer solution is used, the micelles formed a distinct spherical shape and smooth surface without aggregation. The average size of micelles was approximately 120 nm. The morphology and aggregation behavior of micelles at a higher concentration (2 g/L) was also investigated by TEM (Fig 3.6 B). A majority of the micelles aggregated and formed larger nanoparticles due to the change of interfacial energy with some of the micelles precipitating out during the fabrication process. Also, the average size and polydispersity index increased.

The resulting size of micelles formed using 3 different compositions were also determined by DLS. As shown in Table 1, the size of micelles slightly increased from 130 nm to 185 nm as the molecular weight of PPG block length increased. This can be attributed to the change in hydrophobic force and longer hydrophobic PPG block, which exhibited a tendency to secondary or higher level of aggregation and eventually built up bigger core of micelles [62]. The formation of

more stable and smaller particle sizes (<200 nm) would be suitable for anticancer drug delivery applications due to the ability allowing passive tumor-targeting through enhanced permeability and Retention(EPR) effect [63-65]. H40–PLA-b-MPEG/PEG–FA polymeric micelles with diameters in the range of 64–134 nm were reported to successfully target the delivery of chemotherapy treatment for cancer therapy [66]. Therefore, the size range of MPEG-b-PPGCA-cys may be appropriate for tumor-targeted drug delivery. Moreover, at the same concentration, the diameters (185 nm) of MPEG-b-PPG2000CA-cys micelles observed by DLS were slightly larger than those (120 nm) obtained by TEM. This can be explained due to methods used to obtain the particle sizes. The diameters of micelle obtained by DLS was measured by the laser diffraction method (particle-size analyzer), which reflected hydrodynamic diameter of micelles swelling in aqueous solution, while the particles observed by TEM was of the dried micelles [67, 68].

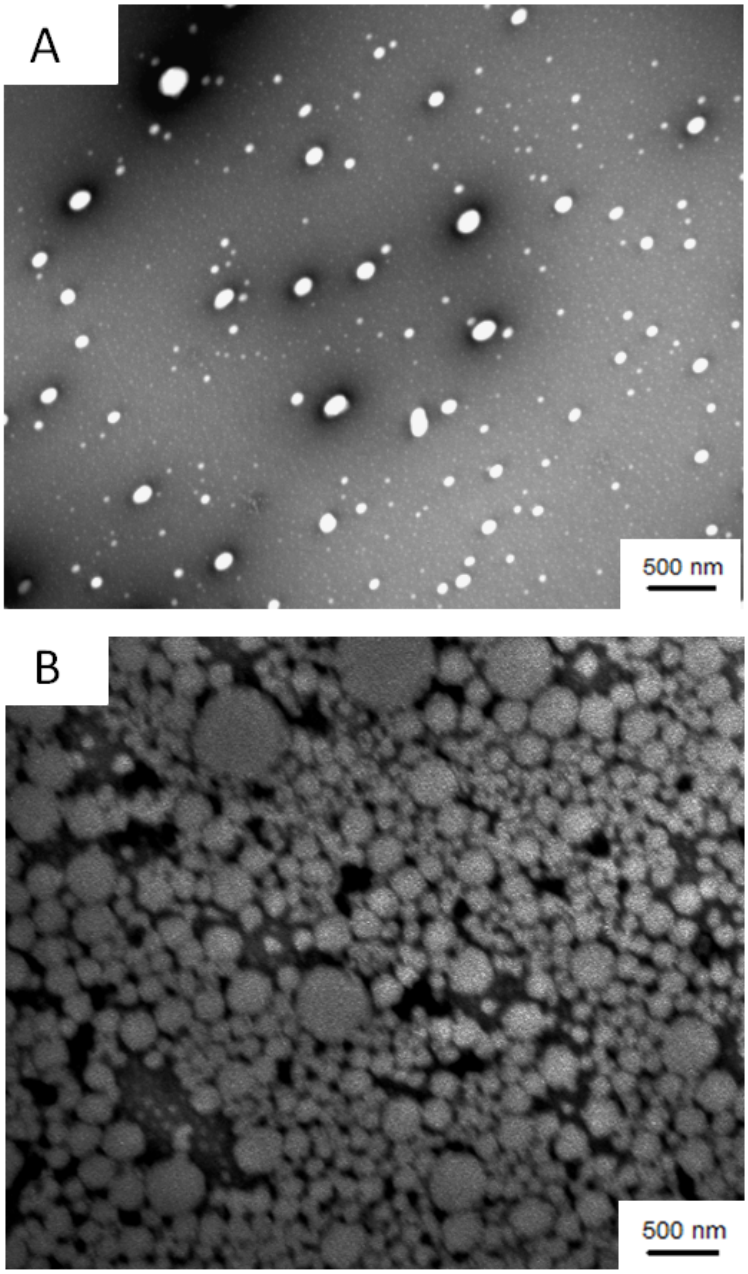

Fig 3.6 TEM micrographs of BPABP (MPEG-b-PPG2000CA-cys) (A) 0.2g/L aqueous solution (B) 2g/L aqueous solution

Table 3.1 CMC values and micelles sizes in aqueous solution for BPABPs (MPEG-b-PPGCA-cys) with various compositions

Micelle aqueous solution	CMC (mg/L)	micelle size in DI water (nm)
PPGCA-MPEG-cys (425)	7.9	130 nm
PPGCA-MPEG-cys (725)	2.5	155 nm
PPGCA-MPEG-cys (2000)	0.1	184 nm

3.4 Photoluminescence Properties of Amphiphilic BPABPs (MPEG-b-PPGCA-cys)

The principle of fluorescence of BPLP families was explored in the previous work [48]. The fluorescence mechanism of the hydrophobic parts of BPLP-PPGCA-cys is similar to that of the previously reported BPLP-cys. According to previous studies, varying the molar concentration of L-cysteine in the polymer, BPLP-POC-cys0.2 was showed the strongest fluorescent intensity [48]. Actually, the fluorescence intensity of BPLP was found to be decreasing with an increasing amount of L-cysteine in the polymer. Therefore, in this study, we only investigated the photoluminescence properties of BPLP-PPGCA-cys0.2 families.

Comparing with regular BPLPs (such as POC-cys), the novel amphiphilic BPABPs (PPGCA-b-MPEG-cys) also showed a strong fluorescence emission (Fig 3.7). In our study, the BPLP-PPGCA-cys0.2 families exhibited the strongest fluorescence emission intensity excited at 360nm. Therefore, all the pre-BPLPs and novel amphiphilic BPABPs families were excited at 360nm, and the excitation and the emission slit widths were set at 1.5nm and 3nm for all samples

unless otherwise stated. The fluorescence intensity of BPLPs-PPGCA-cys0.2 families does not change significantly after conjugating with hydrophilic component MPEG-COOH (Fig 3.8), when dissolved in the solution at same concentration. However, the emission intensity of three types of BPLPs-PPGCA-cys showed a significant difference as seen in Fig 3.8. It can be seen that the high molecular weight hydrophobic PPG2000CA-cys segment emitted the strongest peak when compared with PPG725CA-cys and PPG425-CA-cys. It is well known that conjugated structures can emit fluorescence. The formation of 6-membered rings in the BPLPs reported was an essential structure in the formation of fluorescent polymer based on the previous study. Therefore, the formation of 6-membered rings exposed more in the repeated units when the polymer chains dissolved in the solvent (all the 3 types of BPLP-PPGCA-Cys-0.2 formed by reaction of 1.1:1:0.2 PPG:CA:Cys), if the chains of hydrophobic component PPG become longer (Fig 3.9). From Fig 3.9, it can be seen that the novel photoluminescent amphiphilic block copolymer solution showed a stronger fluorescent intensity when compared to the micelle solution. As we known, the random chains of amphiphilic block copolymer were fully solvated if the polymer completely dissolved in the solvent. In contrast, in the micelles structures, the photoluminescent hydrophobic blocks (fluorophore) aggregated, which bring a possibility for fluorescence quenching.

Furthermore, an artifactual peak was only present in the emission spectra of the micelle. Due to a second-order transmission of diffraction grating monochromator when set to a given wavelength λ, partially transmit light with wavelength λ/2 [69]. For this reason, the excitation

wavelength is set at 360nm, and also produces an artifactual emission peak at 720 nm. From the emission spectra (Fig 3.9), it is hard to see the artifactual emission peak for polymer solution. While the peak of artifactual emission was clearly increased after the micelles structure formed due to a second-order transmission of spacing between micelles. Comparing different concentration of micelles solution, the intensity of the artifactual emission peak decreased as the concentration of the polymer in solution decreased from 0.8g/L to 0.1g/L (Fig 3.10). However, the intensity of artifactual emission peak decreased as the concentration of the polymer in solution increased from 0.8g/L~5g/L (Fig 3.11). It should be noted that the intensity of artifactual emission peak was based on the size of particles. As we suspected, the average size of particles was above 1000nm at high concentration (2g/L~5g/L) due to the aggregation of micelles. On the other hand, the size of self-assembled micelles is only about 150nm at relative low concentration (0.1g/L~0.8g/L). Therefore, the significant artifactual emission intensity was believed to associate with the size and the uniformity of micelles.

The quantum yields of BPABPs families were measured and compared with standard (Fig 3.12). The various forms of BPABPs solution were found to exhibit high quantum yields (44%~55%) comparing with those organic fluorescent protein reported before, such as green fluorescent protein (GFP) (7.3%) [11, 70]. However, the fluorescent quantum yields of micelles solution of BPABPs families were much lower than those of the polymers in dioxane. We suspect that most fluorescent 6-membered rings were encapsulated inside of micelles due to the

aggregation of polymers in aqueous solution. The potential fluorescence quenching may decrease their quantum yields. Nevertheless, the photoluminescent amphiphilic block copolymer micelles also showed strong quantum yields (5%~15%). Moreover, the molar absorption coefficients of BPABPs micelles were much higher than those for BPABPs in dioxane solution. This result indicated that micelles of nanostructure have high capacity of light absorption, though they exhibit relative low quantum yields. All the results of quantum yields and molar absorption coefficient of BPABPs families are listed in Table 3.2.

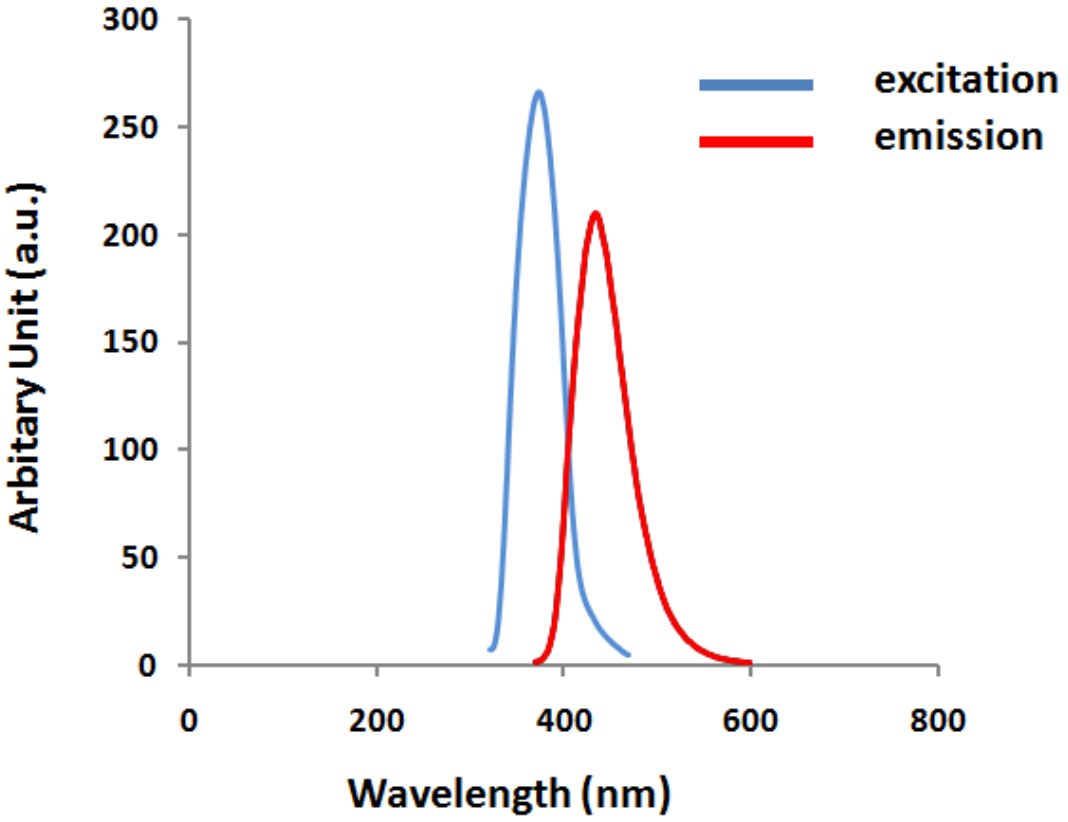

Fig 3.7 Excitation and emission spectra of BPABPs (MPEG-b-PPGCA-cys) solution in dioxane

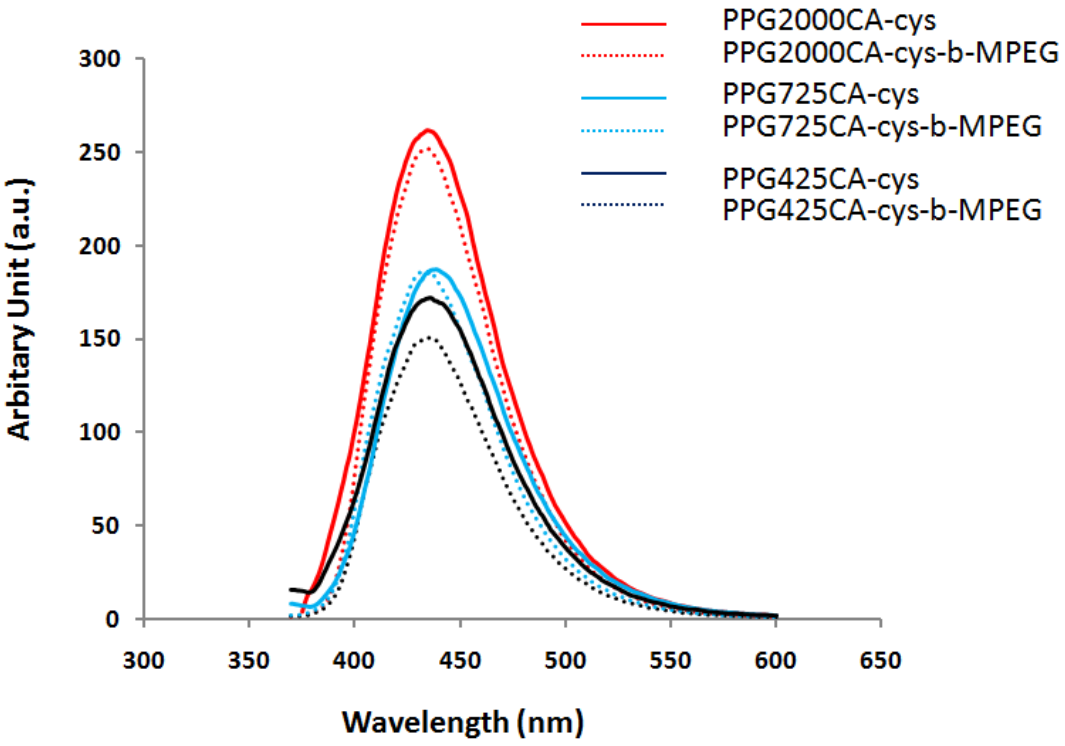

Fig 3.8 Emission spectra of BPABPs (PPGCA-cys and MPEG-b-PPGCA-cys) solution in dioxane.

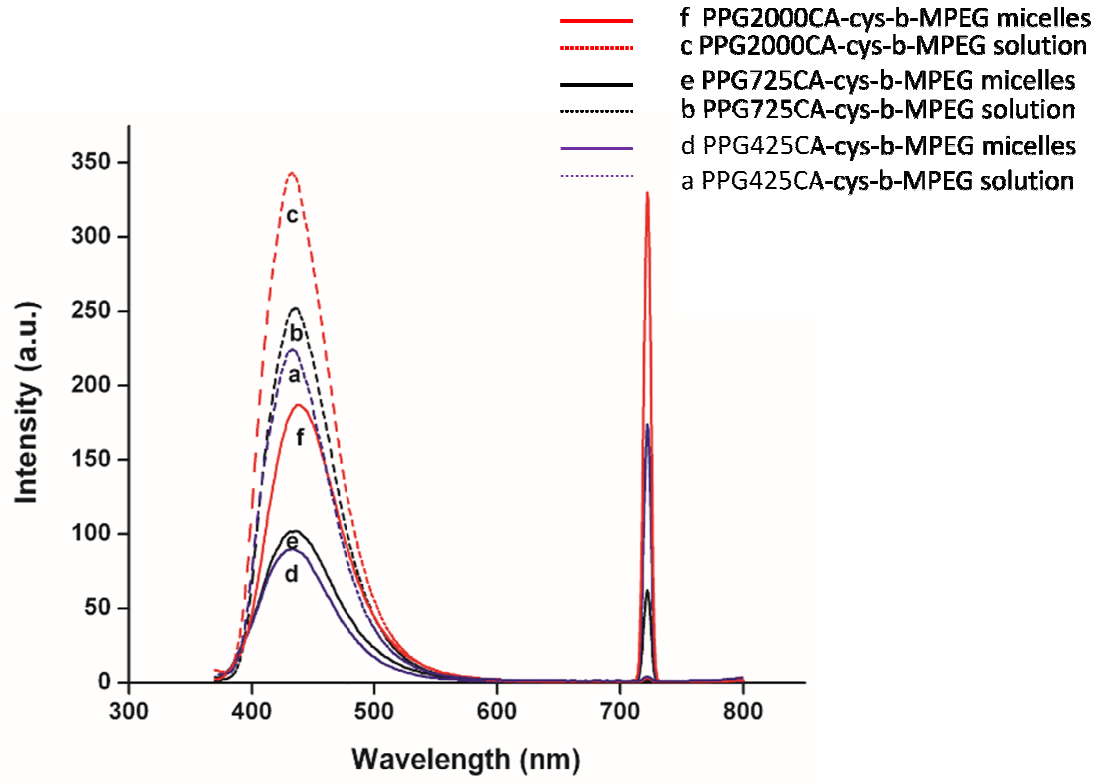

Fig 3.9 Emission spectra of all the 3 types of BPABPs (MPEG-b-PPGCA-cys) solution in dioxane and their micelles solution

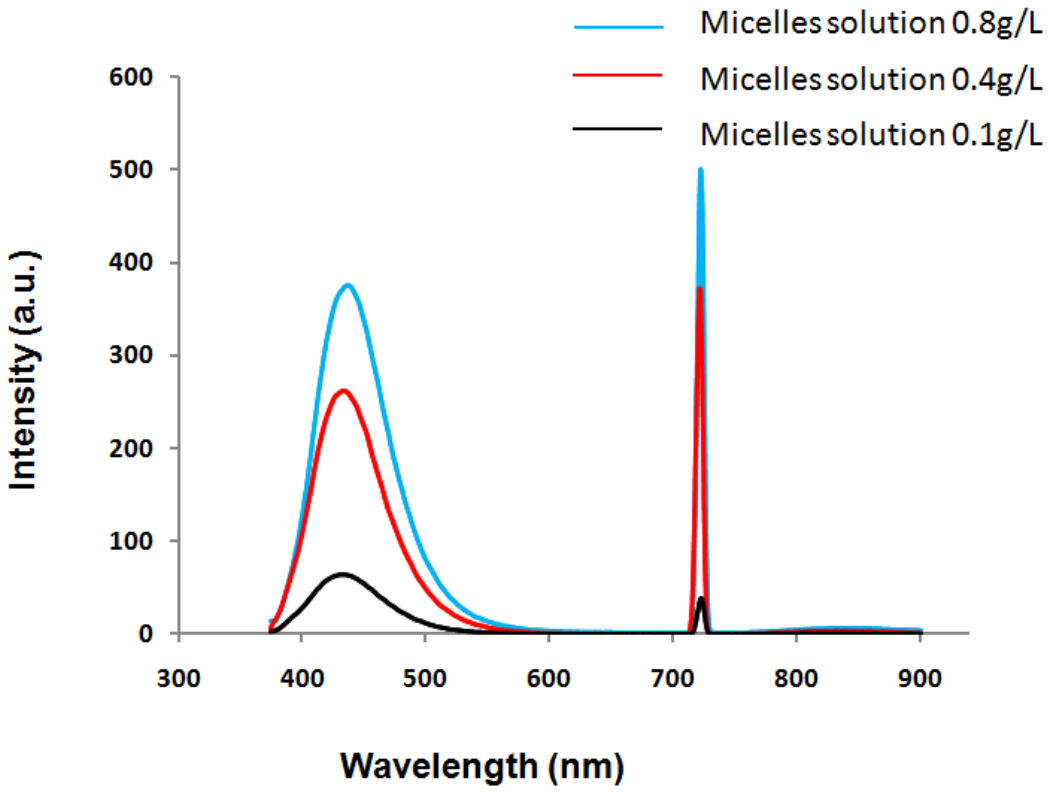

Fig 3.10 Emission spectra of low concentration BPABP (MPEG-b-PPG425CA-cys) micelle solution

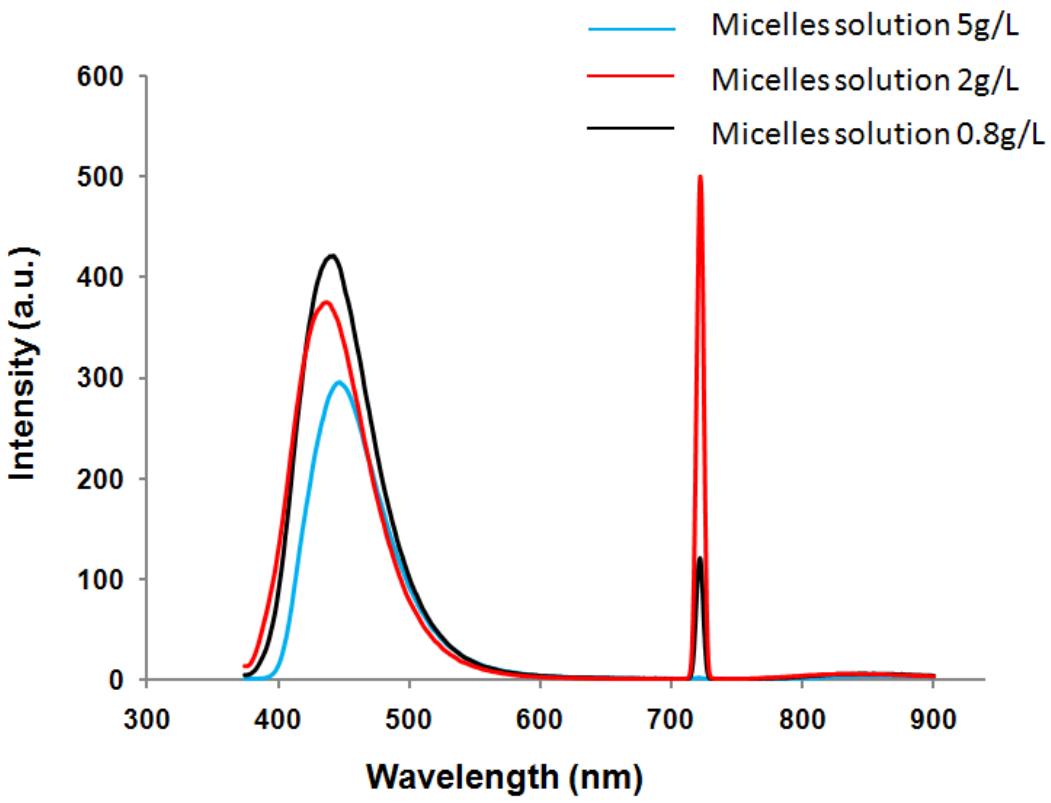

Fig 3.11 Emission spectra of high concentration BPABP (MPEG-b-PPG425CA-cys) micelle solution

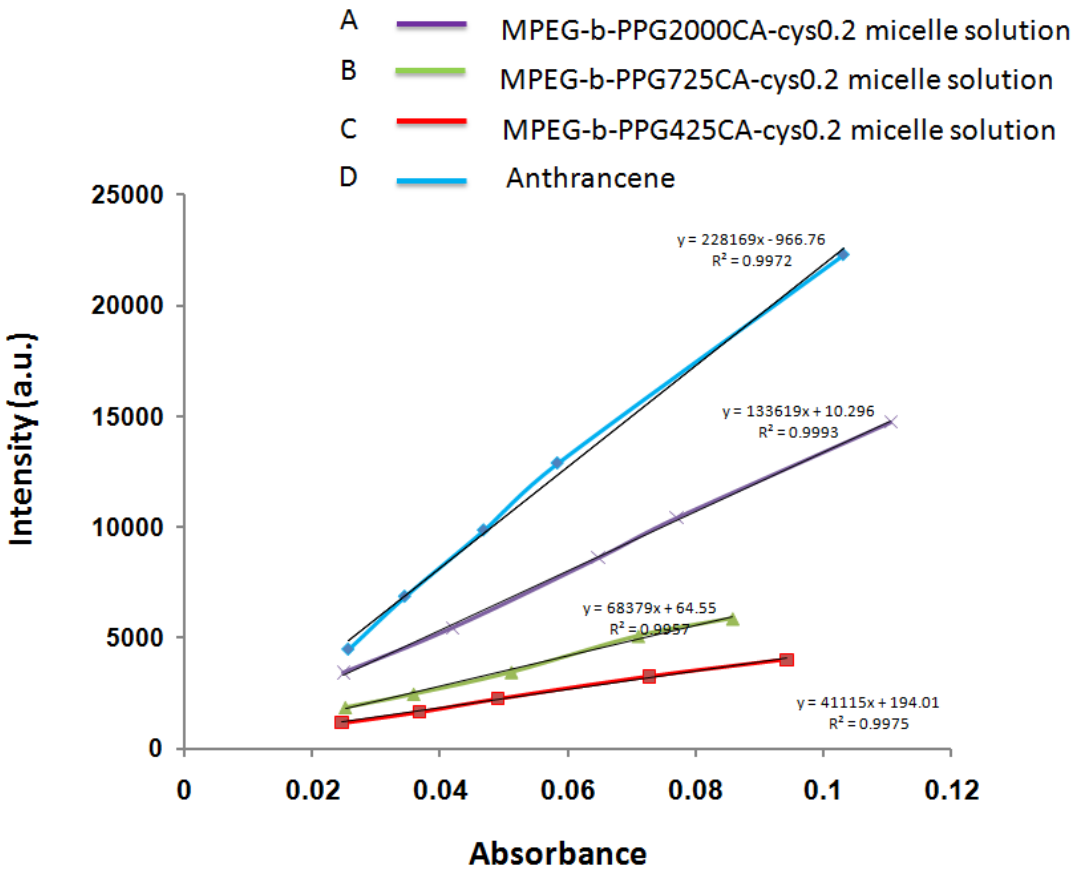

Fig 3.12 Intensity-absorbance curve of BPABPs (MPEG-b-PPGCA-cys) micelles solution for quantum yield measurements

Table 3.2 Quantum yields and molar absorption coefficient of BPABPs (MPEG-b-PPGCA-cys) families

Polymer solution	**QY**	ε, $L \cdot mol^{-1} \cdot cm^{-1}$
PPG425CA1.1-cys0.2-MPEG micelle aqueous solution	0.047	5560
PPG725CA1.5-cys0.2-MPEG micelle aqueous solution	0.072	3560
PPG2000CA1.5-cys0.2-MPEG micelle aqueous solution	0.158	2450
PPG425CA1.5-cys0.2-MPEG dioxane solution	0.553	514.5
PPG725CA1.5-cys0.2-MPEG dioxane solution	0.443	345.9
PPG2000CA1.5-cys0.2-MPEG dioxane solution	0.447	360

BPABPs (PPGCA-cys) families solution (0.2mg/ml in 1,4 dioxane or 0.2mg/ml in deionized water) were used for photoluminescence characterization.

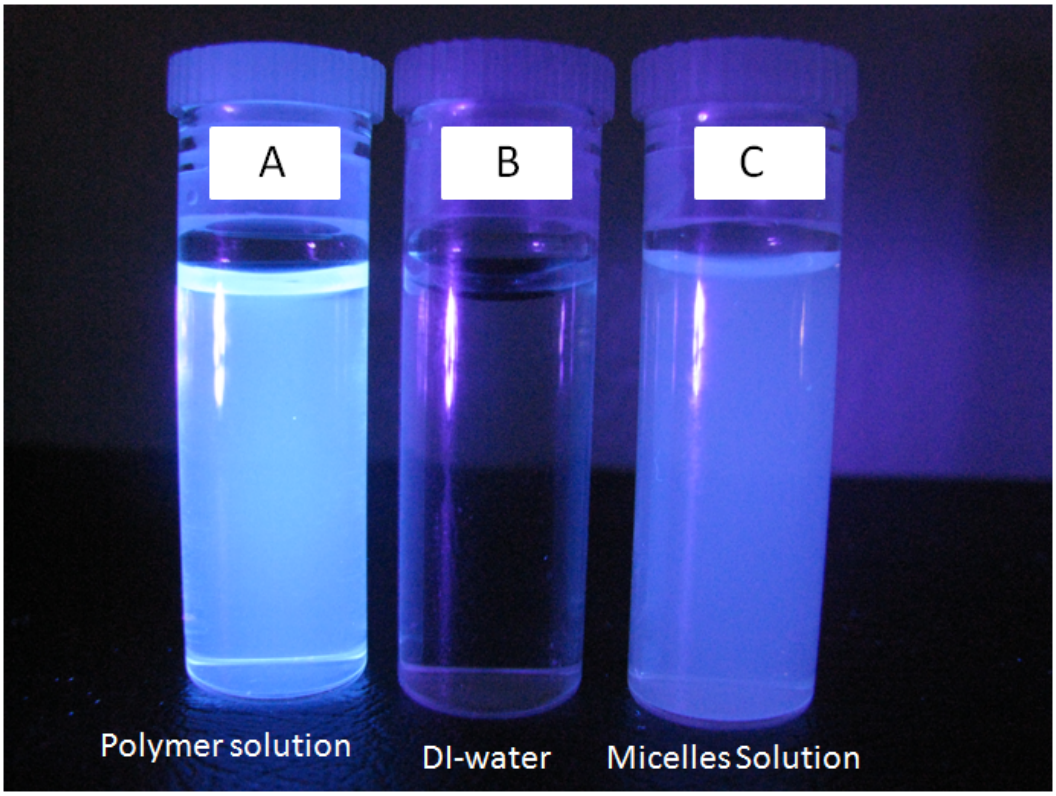

Fig 3.13 Photograph of BPABP (MPEG-b-PPGCA-cys) under UV in dark room (A) Image of BPABP (MPEG-b-PPGCA-cys) dissolved in 1,4-dioxane (B) Image of deionized water (C) Image of BPABP (MPEG-b-PPGCA-cys) micelles in DI-water. DI-water was used as control

3.5 Bioimaging Studies in Vitro

The potential application of novel fluorescent BPABP (MPEG-b-PPGCA-cys) micelles was evaluated for cellular bioimaging in vitro (Fig. 3.14). The images of 3T3 fibroblasts were recorded after treated with the fluorescent micelles. It was found that cells could be labeled with different fluorescence color due the wide emission of BPABP-Cys. The various fluorescence colors also

indicated that micelles retain strong, wide fluorescence emission ranging from blue to red, which provide a potential application of cellular imaging. Compared with the images of in Figures 3.14 (A) and (B) of 3T3 cells, cells survived and no obvious aggregation of micelles was observed during 4 days of uptake. Furthermore, fluorescent micelles also emitted strong, tunable fluorescence ranging from blue to red after 4 days cells uptake. These preliminary data supported good cell compatibility and stability, that are essential for their drug delivery and bioimaging applications.

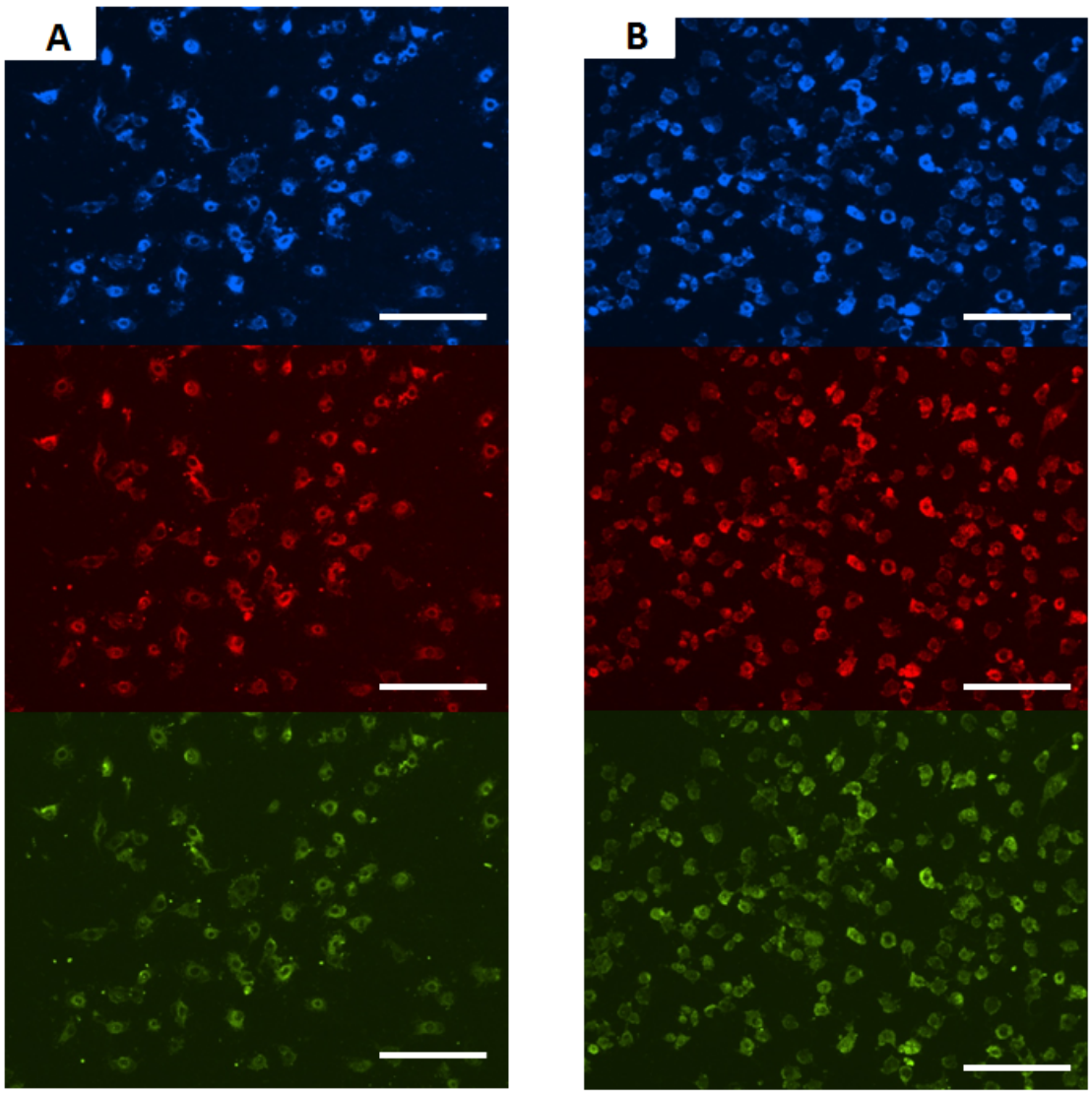

Fig. 3.14 BPABP (MPEG-b-PPGCA-cys) micelles-uptaken 3T3 mouse fibroblasts observed under fluorescent microscope with FITC filter (20×) (A) 24 hours after uptake (B) 4 days after uptake (scale bar 100 μm).

3.6 In Vitro Cytotoxicity

As an effective and appropriate drug delivery vehicle, cytotoxicity is an important factor we need to consider. We used NIH 3T3 fibroblasts as model cells to evaluate the cytotoxicity of BPABP (MPEG-b-PPGCA-cys) micelles. The cell viability was evaluated (Fig 3.15) after 24 h incubation in BPABP (MPEG-b-PPGCA-cys) micelle solutions (MPEG-b-PPG425CA-cys, MPEG-b-PPG725CA-cys and MPEG-b-PPG2000CA-cys) at different concentrations using MTT assays. MPEG-b-PPG2000CA-cys exhibited the lowest toxicity among these groups. Even when the concentration is up to 1 g/L, the viability of cells also remains (>75%). The cell viability remain nearly 90% when concentration of micelles is 0.1g/L. Actually, the concentration of micelles is below 0.1g/L in extremely dilute state of biological fluids after intravenous administration [56, 57]. The presence of fluorescent micelles did not obviously inhibit the viability of cells. Our results revealed that the novel fluorescent micelles are biocompatible and possessgreat potential for in vivo uses.

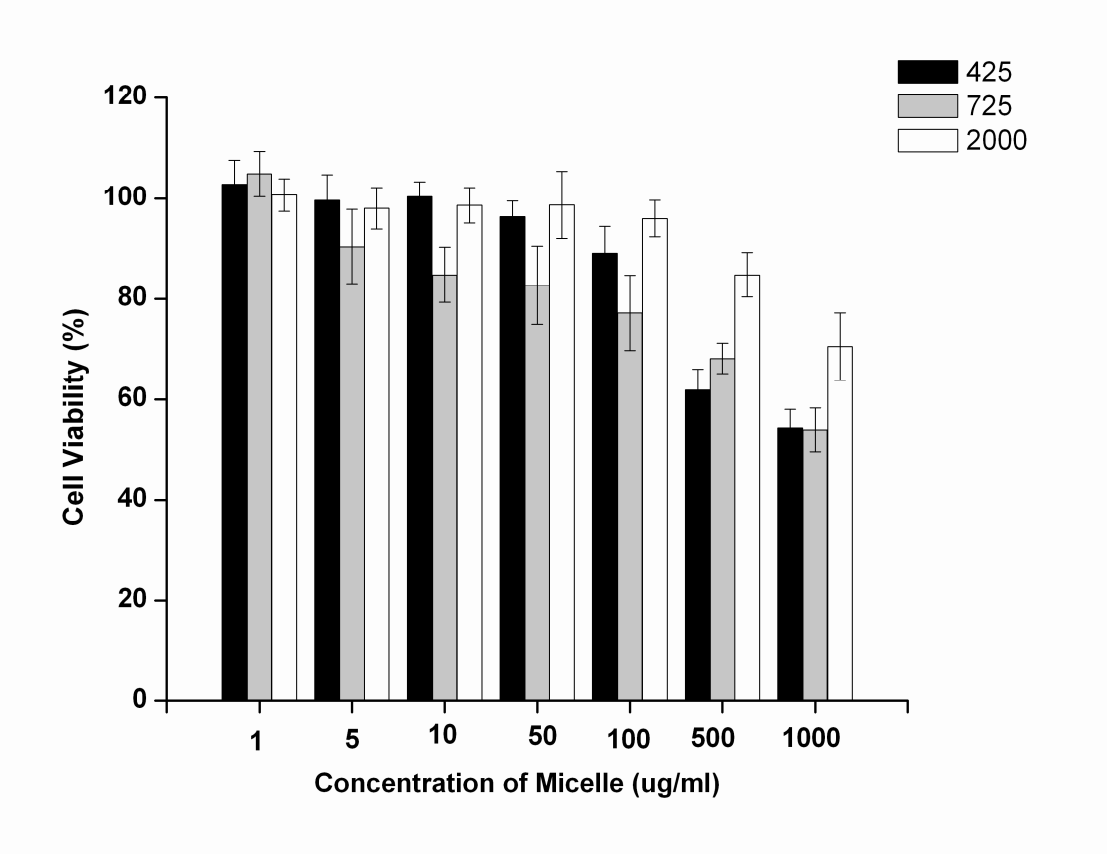

Fig. 3.15 Cytotoxicity evaluation of NIH-3T3 cells treated with various concentrations of micelles solution for 24 h using MTT viability assay. Various compositions of polymeric micelles were evaluated (MPEG-b-PPG425CA-cys, MPEG-b-PPG725CA-cys, and MPEG-b-PPG2000CA-cys).

3.7 Drug Release Study

The amount of drug encapsulated in BPABP (MPEG-b-PPGCA-cys) micelles was measured by an UV–visible spectrophotometer. The block copolymer and 5-Fu are dissolved in DMF followed by dialysis of the solution against water. After centrifugation, the content of 5-FU within micelles was evaluated based on the absorbance of drug present in the supernatant at a wavelength of 270 nm. The drug loading efficiencies depending on various compositions of block polymer is shown in Table 3.3. As shown in Table 3.3, the drug loading efficiency slightly increased with the increase of hydrophobic chain lengths of the block copolymers. In order to evaluate the feasibility of using MPEG-b-PPGCA-cys copolymer as an anticancer drug delivery carrier, in vitro drug release studies were performed in PBS solution (PH 7.4) at 37 ℃. The drug release profiles of 5-Fu incorporated into various compositions of micelles were shown in Fig 3.16. The result suggested that 5-Fu loaded MPEG-b-PPGCA-cys presented an initial burst release(~50% of the initial loading amount) in the first stage (up to 8 h), followed by a sustained release period (up to 40–70 h), and polymeric micelles with different compositions exhibited similar behavior of release. At the first 8 hours, the relative rapid initial burst release of 5-Fu drug from the MPEG-b-PPGCA-cys micelles should be attributed to the drug molecules located within the hydrophilic shell or at the interface between the unimolecular micelles [71]. The release

behavior is mainly dominated by diffusion-controlled mechanism. However, after 8 h burst release stage, the sustained release of the drug from micelles could be attributed to the hydrophobic–hydrophobic interactions between the hydrophobic cores of the polymeric micelles and the hydrophobic drug molecules, which indicated that the few drugs had access to the surrounding hydrophilic corona. Most of the drug loading could be entrapped or even dissolved in the dense aggregation regions of the hydrophobic cores of micelles where polymer chain entanglements provide a much better barrier to drug transport [72, 73].

Table 3.3 5-Fu loading contents of BPABP family micelles

	MPEG-b-PPG425-CA-cys	**MPEG-b-PPG725-CA-cys**	**MPEG-b-PPG2000-CA-cys**
DLE	16.92%	17.25%	19.14%

DLE means Drug Loading Efficiency (%).

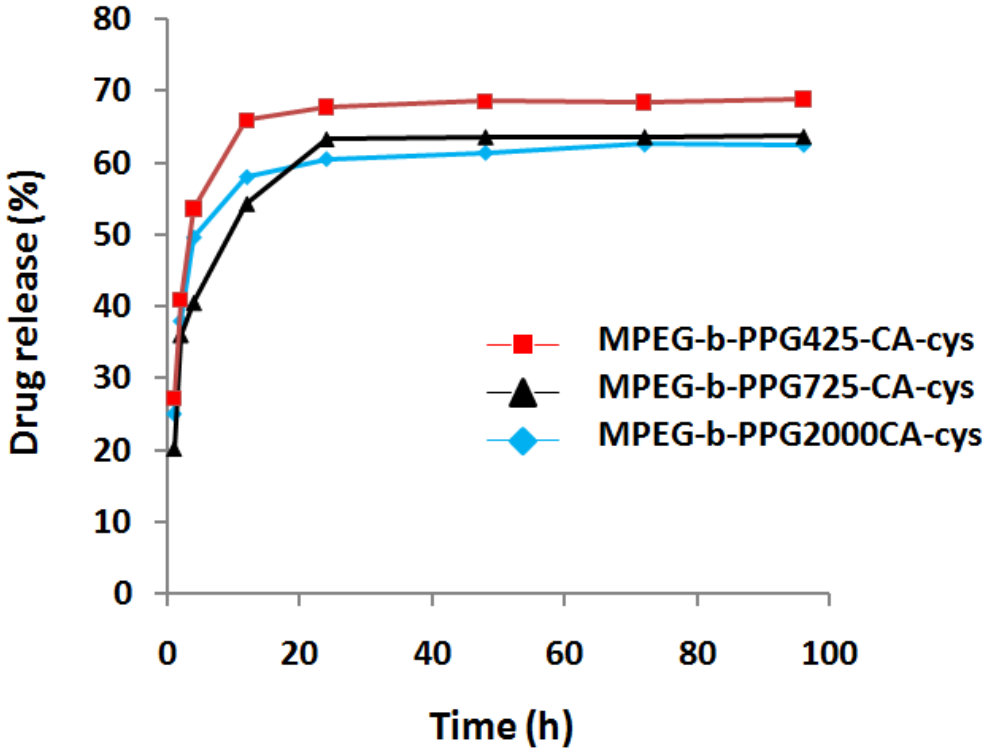

Fig. 3.16 5-Fu release from 5-FU-loaded BPABPs (MPEG-b-PPGCA-cys) micelles with various compositions

CHAPTER 4

CONCLUSIONS

In this research work, a family of novel biodegradable photoluminescent amphiphilic block polymer, BPABPs (MPEG-b-PPGCA-cys) were successfully prepared. All these polymers can spontaneously self-assembled into micelles in aqueous environment, when the concentration of polymers is above CMC. The relative low CMC value of polymeric micelles indicated that the self-assembled micelles could remain stable in dilute situations, and also demonsrated long-term stability. The CMC value can be controlled by varying the hydrophobic chains of polymers. The size of micelles ranged from 120 to 180nm. The drug release profile of 5-FU-loaded MPEG-b-PPGCA-cys micelles showed an initial burst release followed by a sustained release period (up to 70 h). All these mentioned results exhibited that the self-assembled micelles from BPABP (MPEG-b-PPGCA-cys) may be a suitable candidate serving as drug delivery carriers. Considering the unique photoluminescent properties of polymers, the fluorescent properties of polymer solution and polymeric micelles aqueous solution were determined and compared. The results suggested that polymeric micelles solution also showed broad emission range and higher quantum yield compared to the fluorescent proteins. A significant artifactual emission peak was believed to associate with the size and uniformity of the self-assembled micelles. The presence of

such artifactual peaks are also a sign of nano-scale micelle formation. The cellular uptake of fluorescent micelles and imaging studies demonstrated their potential for cellular imaging applications. In addition, these novel fluorescent micelles preliminarily showed excellent biocompatibility and photostability during 4 days cells uptake. In conclusion, the development of novel biodegradable photoluminescent amphiphilic block polymer promises a new direction and future in biomedical field for serving as bioimaging probes and vehicles of drug delivery in vitro and vivo.

CHAPTER 5

LIMITATIONS AND FUTURE WORK

The goal of this project was to develop novel biodegradable photoluminescent amphiphilic block polymer. The characterization of polymers, evaluation of photoluminescent property and self-assembled behavior of polymers were only initial steps to explore polymers of this family. Though this amphiphilic BPABP family showed some advantage as bioimaging labels and vehicle of drug delivery in vitro, the potential limitation are discussed below.

5.1 Limitations

- Polymeric micelles exhibited a relative lower quantum yield compared to polymer solution, though polymeric micelles showed higher molar absorption coefficients in aqueous solution.
- The drug loading efficiency is less 20% and the sustained release period of 5-FU was limited.
- The size stability and photostability of micelles have not been evaluated in long time.

5.2 Future Work Recommendations

- The degradation of polymeric micelles should be considered and evaluated in a longer term.
- The in vivo implantation study and imaging study of micelles might be a significant step to further evaluate the biocompatibility of polymers and their potential use as bioimaging probes.
- The micelles size stability and photostability of micelles can be investigated.
- BPABPs can be modified though conjugation with fluorescent hydrophilic segment. The investigation of dual fluorescent amphiphililic structures will provide new paths to generate new opportunities for biomedical applications.

REFERENCES

1. M. Yokoyama, G. S. Kwon, T. Okano, Y. Sakurai, T. Seto, K. Kataoka. Bioconjugate Chem. 3, 295–301 (1992).

2. K. Kataoka, G. S. Kwon, M. Yokoyama, T. Okano, Y. Sakurai. J. Controlled Release 24, 119–132 (1993).

3. G. S. Kwon and T. Okano. Adv. Drug Delivery Rev. 21, 107–116 (1996).

4. T. S. Wiedmann and L. Kamel. J. Pharm. Sci. 91, 1743–1764 (2002).

5. K. Kataoka, A. Harada, Y. Nagasaki. Adv. Drug Delivery Rev. 47,113–131 (2001).

6. G. S. Kwon. Adv. Drug Delivery Rev. 54, 167 (2002).

7. Zhang, L.; Eisenberg, A. Science (1995), 268, 1728–1745.

8. H. Liu, S. Farrell, and K. Uhrich. (2000). Drug release characteristics of unimolecular polymeric micelles. J. Control. Release 68:167–174

9. Nasongkla N, Bey E, Ren J, Ai H, Khemtong C, Guthi JS, et al. (2006) Multifunctional polymeric micelles as cancer-targeted, MRI-ultrasensitive drug delivery systems. Nano Letters; 6:2427–30.

10. M.H. Dufresne, E. Fournier, M.-C. Jones, M. Ranger, (2003) Block copolymer micelles—engineering versatile carriers for drugs and biomacromolecules, in: R. Gurny (Ed.), B.T. Gattefosse, vol. 96, Gattefosse, Saint-Priest, pp. 87–102.

11. Tsien RY. (1998) The green fluorescent protein. Annual Review of Biochemistry. 67: p. 509-44.

12. Mena MA, Treynor TP, Mayo SL, Daugherty PS. (2006) Blue fluorescent proteins with enhanced brightness and photostability from a structurally targeted library. Nature Biotechnology. 24(12): p. 1569-71.

13. Li H, Shih WY, Shih WH. (2007) Non-heavy-metal ZnS quantum dots with bright blue photoluminescence by a one-step aqueous synthesis. Nanotechnology, 18(20): p. 205604-1.

14. Chan WC, Maxwell DJ, Gao X, Bailey RE, Han M, Nie S. (2002) Luminescent quantum dots for multiplexed biological detection and imaging. Current Opinion in Biotechnology,. 13(1): p. 40-6.

15. Pinaud F, Michalet X, Bentolila LA, Tsay JM, Doose S, Li JJ, Iyer G, Weiss S. (2006) Advances in fluorescence imaging with quantum dot bio-probes. Biomaterials,. 27(9): p. 1679-87.

16. Duncan R. (2003) The dawning era of polymer therapeutics. Nat Rev Drug Discov 2:347–60.

17. Han S,Mahato RI, Sung YK, Kim SW. (2000) Mol Ther; 2:302. 515

18. Kwon GS, Kataoka K. (1995) Block copolymer micelles as long-circulating drug vehicles. Adv Drug Deliv Rev; 16:295–309.

19. Park TG, Jeong JH, Kim SW. (2006) Current status of polymeric gene 518 delivery systems. Adv Drug Deliv Rev; 58:467.

20. C. Allen, D. Maysinger, and A. Eisenberg. (1999) Nano-engineering block copolymer aggregates for drug delivery. Coll. Surf. B: Biointerf. 16:1–35.

21. Kim KH, Cui GH, Lim HJ, Huh J, Ahn CH, Jo WH. (2004) Synthesis and micellization of star-shaped poly(ethylene glycol)-block-poly (epsilon-caprolactone). Macromo Chem and Phys; 205: 1684-92.

22. Deng MX, Chen XS, Piao LH, Zhang XF, Dai ZL, Jing XB. (2004) Synthesis of four-armed poly(epsilon-caprolactone)-block-poly(ethylene oxide) by diethylzinc catalyst. J Polym Sci Part a-Polym Chem; 42: 950-59.

23. Allen C, Han J, Yu T, Maysinger D, Eisenberg A. (2000) Polycaprolactone-b-poly(ethylene oxide) copolymer micelles as a delivery vehicle for dihydrotestosterone. J Control Release; 63: 275-86.

24. Lim Soo P, Luo L, Maysinger D, Eisenberg A. (2002) Incorporation and Release of Hydrophobic Probes in Biocompatible Polycaprolactone-block-poly(ethylene oxide) Micelles: Implications for Drug Delivery. Langmuir; 18: 9996-10004.

25. Yokoyama M, Satoh A, Sakurai Y, Okano T, Matsumura Y, Kakizoe T, et al. (1998) Incorporation of water-insoluble anticancer drug into polymeric micelles and control of their particle size. J Control Release; 55: 219-29.

26. M.J. Lawrence, (1994) Surfactant systems-their use in drug delivery Chem. Soc. Rev. 23 417–424.

27. F. Wang, T.K. Bronich, A.V. Kabanov, R.D. Rauh, J. Roovers, et al. (2008) Synthesis and characterization of star poly(epsilon-caprolactone)-b-poly(ethylene glycol) and poly(L-lactide)-b-poly(ethylene glycol) copolymers: Evaluation as drug delivery carriers. Bioconjugate Chem.19 1423–1429.

28. Kreutzer, G; Ternat, C; Nguyen, TQ, et al. (2006) Water-soluble, unimolecular containers based on amphiphilic multiarm star block copolymers. Macromolecules 39: 4507–4516.

29. Santosh Aryal, Mani Prabaharan, (2009) Biodegradable and biocompatible multi-arm star amphiphilic block copolymer as a carrier for hydrophobic drug delivery. International Journal of Biological Macromolecules 44: 346-352

30. K.B. Thurmond II, H. Huang, C.G. Clark Jr., T. Kowalewski and K.L. Wooley, (1999) Shell cross-linked polymer micelles: stabilized assemblies with great versatility and potential, Colloids Surf., B **16**, pp. 45–54.

31. X. Shuai, T. Merdan, A.K. Schaper, F. Xi and T. Kissel, (2004) Core-cross-linked polymeric micelles as paclitaxel carriers, Bioconjug. Chem. 15, pp. 441–448.

32. Yoo HS, Park TG. (2001) Biodegradable polymeric micelles composed of doxorubicin conjugated PLGA-PEG block copolymer. J Control Release; 70: 63-70.

33. Shuai XT, Ai H, Nasongkla N, Kim S, Gao JM. (2004) Micellar carriers based on block copolymers of poly(e-caprolactone) and poly(ethylene glycol) for doxorubicin delivery. J Control Release; 98: 415-26.

34. Alakhov V, Klinski E, Li S, Pietrzynski G, Venne A, Batrakova E,et al. (1999) Block copolymer-based formulation of doxorubicin. From cell screen to clinical trials. Colloids Surf B Biointerfaces; 16: 113-34.

35. Shuai X, Merdan T, Schaper AK, Xi F, Kissel T. (2004) Core-cross-linked polymeric micelles as paclitaxel carriers. Bioconjug Chem; 15: 441-8.

36. Liggins RT, Burt HM. (2002) Polyether-polyester diblock copolymers for the preparation of paclitaxel loaded polymeric micelle formulations. Adv Drug Deliv Rev; 54: 191-202

37. Pan Jie, Subbu S. Venkatraman. (2005) Micelle-like nanoparticles of star-branched PEO–PLA copolymers as chemotherapeutic carrier. Journal of Controlled Release 110: 20– 33

38. Yuan Li, Xian RongQi. (2009) PEG–PLA diblock copolymer micelle-like nanoparticles as all-trans-retinoic acid carrier: in vitro and in vivo characterizations. Nanotechnology 20 055106

39. Jinyoung Ko, et al. (2007) Tumoral acidic extracellular pH targeting of pH-responsive MPEG-poly(β-amino ester) block copolymer micelles for cancer therapy Journal of Controlled Release 123: 109-115

40. Zollinger, H. (2003). Color Chemistry. Synthesis, Properties and Applications of Organic Dyes and Pigments, 3rd ed. Weinheim: Wiley-VCH.

41. Bruchez, M., Jr.; Moronne, M.; Gin, P.; Weiss, S.; Alivisatos, A.P. (1998) Semiconductor Nanocrystals as Fluorescent Biological Labels. Science, 281, 2013-2016.

42. Parak WJ, Gerion D, Pellegrino T, Zanchet D, Micheel C, Williams SC, Boudreau R, Le Gros MA, Larabell CA, Alivisatos AP.(2003) Biological applications of colloidal nanocrystals. NANOTECHNOLOGY 14: 15-27

43. Larson DR, Zipfel WR, et al. (2003) Water-soluble quantum dots for multiphoton fluorescence imaging in vivo. Science 300: 1434-1436

44. Medintz IL, Uyeda HT, et al. (2005) Quantum dot bioconjugates for imaging, labelling and sensing. Science 4: 435-446

45. R. Vogel, M. Harvey, G. Edwards, P. Meredith, N. Heckenberg, M. Trau, H. (2002) Rubinsztein-Dunlop, Macromolecules 35 2063.

46. Y. Li, L.-J. Ding, Y.-K. Gong, K. Nakashima, Journal of Photochemistry and Photobiology A: Chemistry 161 (2004) 125–129

47. Saswati Basua, Samiran Mondala, Uma Chatterjeeb, Debabrata Mandala,∗, Materials Chemistry and Physics 116 (2009) 578–585

48. Jian Yang, Yi Zhang, Santosh G, Proc. Nat. Acad. Sci. USA , 2009 106:10086-10091.

49. Hersel U, Dahmen C, Kessler H (2003) RGD modified polymers: biomaterials for stimulated cell adhesion and beyond. Biomaterials 24:4385–4415

50. Rapoport N (2007) Physical stimuli-responsive polymeric micelles for anti-cancer drug delivery. Prog Polym Sci 32:962–990

51. Dubertret B, Skourides P, et al. (2002) In vivo imaging of quantum dots encapsulated in phospholipid micelles. Sicence 298: 1759-1762

52. F. M. Winnik and S. T. A. Regismond. In Polymer-Surfactant Systems, I. C. T. Kwak (Ed.), pp. 267–315, Marcel Dekker, New York (1998).

53. K. Kalyanasundaram and J. K. Thomas. J. Am. Chem. Soc. 99, 2039–2044 (1977).

54. Williams ATR, Winfield SA, Miller JN (1983) Relative fluorescence quantum yields using a computer-controlled luminescence spectrometer. Analyst 108:1067–1071.

55. Allen, C.; Maysinger, D.; Eisenberg, A. Colloid Surf B Biointerf 1999, 16, 3.

56. Nichole F.; Bryan H, and Christine Allen, Biomacromolecules, 2008, 9 (9), 2283-2291

57. Savic, R.; Eisenberg, A.; Maysinger, D. J. Drug Targeting 2006, 14, 343–355.

58. Astafieva, I.; Zhong, X.; Eisenberg, A. Macromolecules 1993, 26, 7339–7352.

59. R. Nagarajan and K. Ganesh. Macromolecules 22, 4312–4325 (1989).

60. Li, YY; Zhang, XZ; Cheng, H, (2007) Fluorescent, thermo-responsive biotin-P(NIPAAm-co-NDAPM)-b-PCL micelles for cell-tracking and drug delivery. NANOTECHNOLOGY 18 505101

61. Patist A, Kanicky J R, Shukla P K ; (2002) Importance of micellar kinetics in relation to technological processes J. Colloid Interface Sci. 245 1-15

62. Muhmud A, Xiong XB, Lavasanifar A. (2008) Development of novel polymeric micellar drug conjugates and nano-containers with hydrolyzable core structure for doxorubicin delivery. European Journal of Pharmaceutics and Biopharmaceutics;69:923–34.

63. Yuan F, Dellian M, Fukumura D, Leunig M, Berk DA, Torchilin VP, et al. (1995) Vascular permeability in a human tumor xenograft: molecular size dependence and cutoff size. Cancer Research;55:3752–6.

64. Schmalenberg KE, Frauchiger L, Nikkhouy-Albers L, Uhrich KE. (2001) Cytotoxocity of a unimolecular polymeric micelle and its degradation products.Biomacromolecules;2:85 1–5.

65. Davis SS, Illum L. (1988) Polymeric microspheres as drug carriers. Biomaterials; 9:111–5.

66. Mani Prabaharan a, Jamison J. Grailer b, Srikanth Pilla (2009) a, Folate-conjugated amphiphilic hyperbranched block copolymers based on Boltorn H40, poly(L-lactide) and poly(ethylene glycol) for tumor targeted drug delivery. Biomaterials 30 3009–3019

67. Morita T, Horikiri Y, Suzuki T and Yoshino T (2001) Preparation of gelatin microparticles by co-lyophilization with poly(ethylene glycol): characterization and application to entrapment into biodegradable microspheres Int. J. Pharm. 219 127-137

68. Ye Q, Zhang ZC, Jia HT (2002) Formation of monodisperse polyacrylamide particles by radiation-induced dispersion polymerization: Particle size and size distribution J. Colloid Interface Sci. 253 279-284

69. J. R. Lakowicz, (2006) Principles of Fluorescence Spectroscopy, Springer, Berlin, , pp. 37, 41–44, 55–56, 282.

70. Patterson, GH; Knobel, SM; Sharif, WD, (1997) Use of the green fluorescent protein and its mutants in quantitative fluorescence microscopy. Biophysical J 73: 2782-2790

71. Allen C, Maysinger D, Eisenberg A. (1999) Nano-engineering block copolymer aggregates for drug delivery. Colloids and Surfaces B Biointerfaces;16:3–27.

72. Blanco E, Bey EA, Dong Y, Weinberg BD, Sutton DM, Boothman DA, et al. (2007) β-Lapachone-containing PEG–PLA polymer micelles as novel nanotherapeutics against NQO1-overexpressing tumor cells. Journal of Controlled Release;122:365–74.

73. Liua H, Farrell S, Uhricha K. (2000) Drug release characteristics of unimolecular polymeric micelles. Journal of Controlled Release; 68:167–74.

BIOGRAPHICAL INFORMATION

Shengyuan Zhou was born in Daqing, China in Nov. of 1985. He received his B.S. in Material Science and Engineering in July of 2008 in his hometown and came to the United States in 2008 for his further education. Then, he attended the University of Texas at Arlington in August as a master student in material science and engineering. However, he was immediately attracted to the Biomedical Engineering at joint program of University of Texas at Arlington and University of Texas Southwestern Medical Center. Based on his interests, he joined the Biomaterials and Tissue Engineering Research Laboratory at UTA to work under Dr. Jian Yang. After completion of his Master of Science degree in July of 2010, He is looking forward to find a satisfactory job that fits his academic background in biomedical field.